

Mads Bertelsen, ESS DMSC  
Kim Lefmann, University of Copenhagen

# Virtual experiments

2019 CSNS  
*McStas*  
*School*

*McStas*  
—  —



# Overview of Simulation packages

- McStas
- VITESS
- RESTRAX – back tracking
- MCViNE – uses some McStas
- Older packages  
  MSCAT / NISP / IDEAS
- General-purpose
- Standard tools of the trade

2019 CSNS  
*McStas*  
*School*

*McStas*  
—  —



# Citation analysis

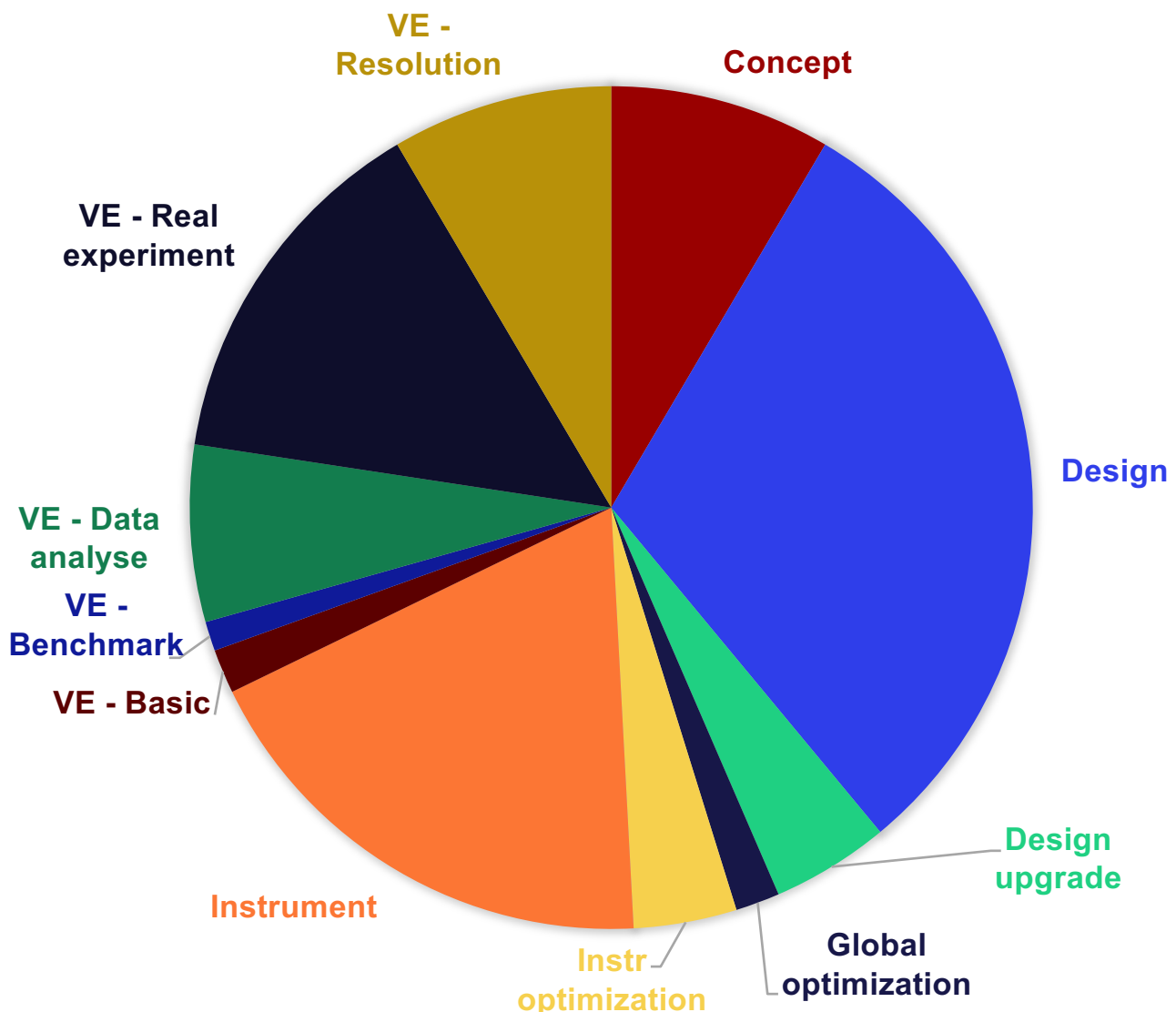
- Package use assessed from citations to package papers
- Excludes papers on:
  - Software tools
  - Components
  - Optics
- 176 papers in analysis
- Concept, design and optimization: 49%
- Instrument paper: 19%
- Virtual experiments: 32%

2019 CSNS  
*McStas*  
School

*McStas*  
n →

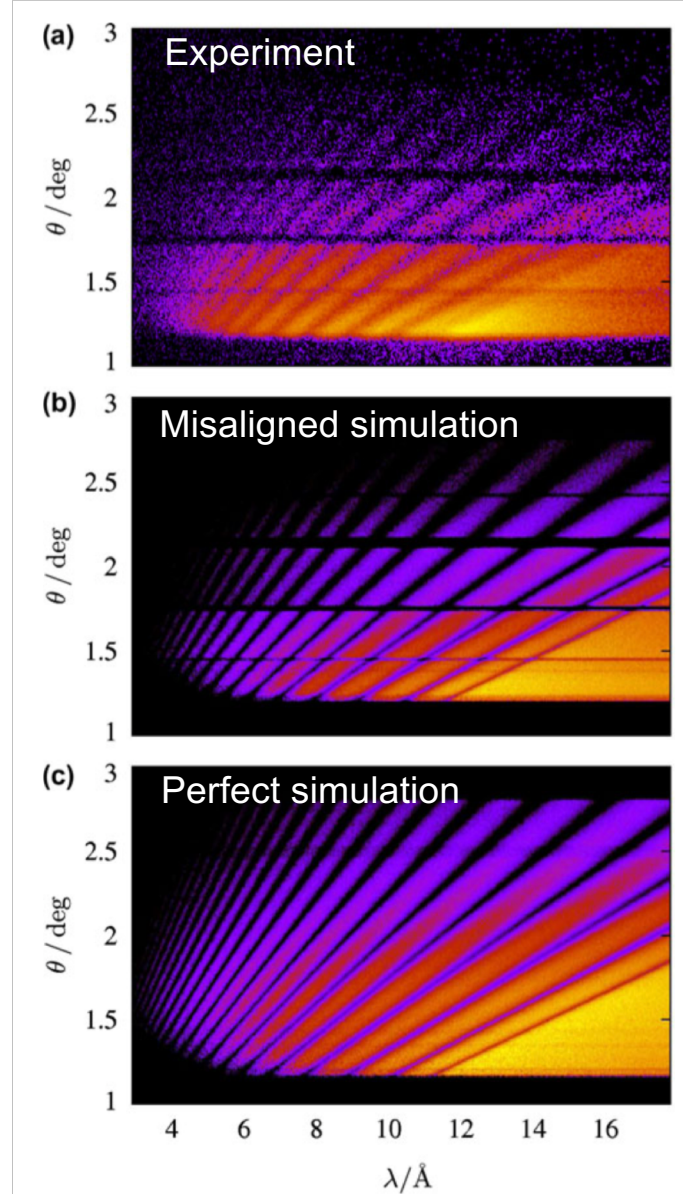
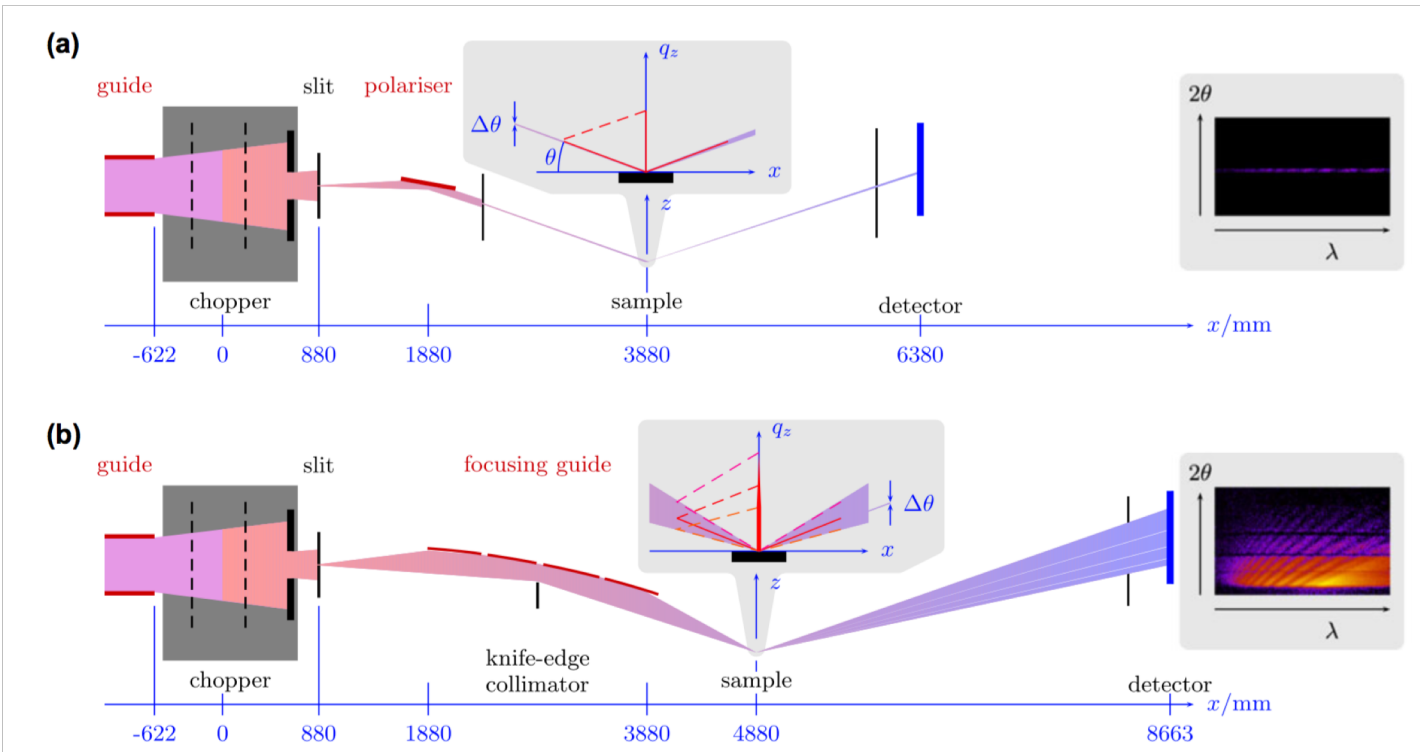


## PUBLICATIONS CITING SIMULATION PACKAGES



# Concepts and design – SELENE on Amor

- Amor @ PSI, 100 nm Ni film measurement

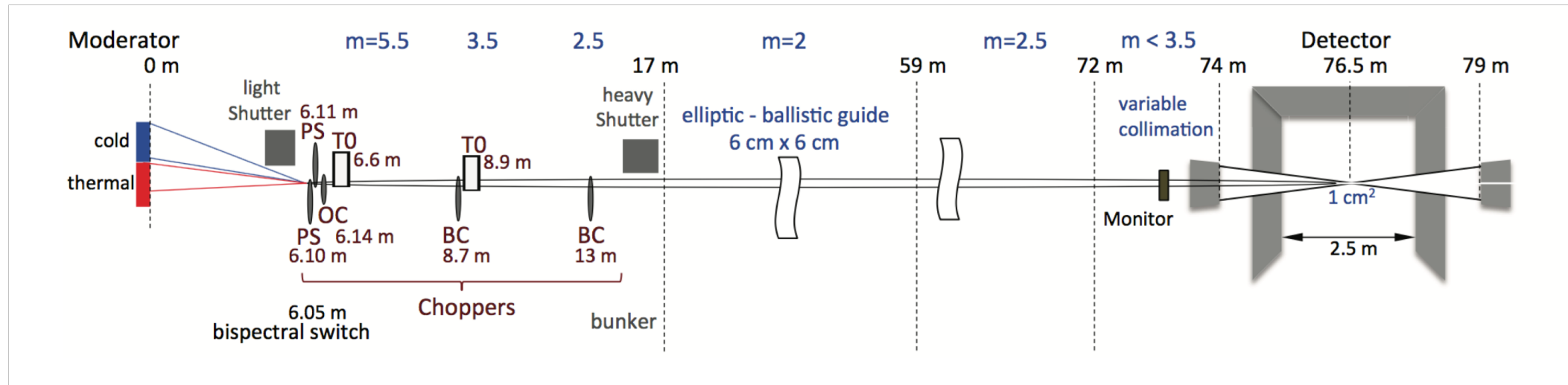


J. Stahn, U. Filges and T. Panzner.

Eur. Phys. J. Appl. Phys. (2012) 58: 11001

# Concepts and design – DREAM ESS Instrument design

- Instrument accepted for construction
- Design presented in paper using VITESS



W Schweika, N Violini, K Lieutenant, C Zendler, D Nekrassov, A Houben, P Jacobs and P F Henry

2016 J. Phys.: Conf. Ser. 746 012013

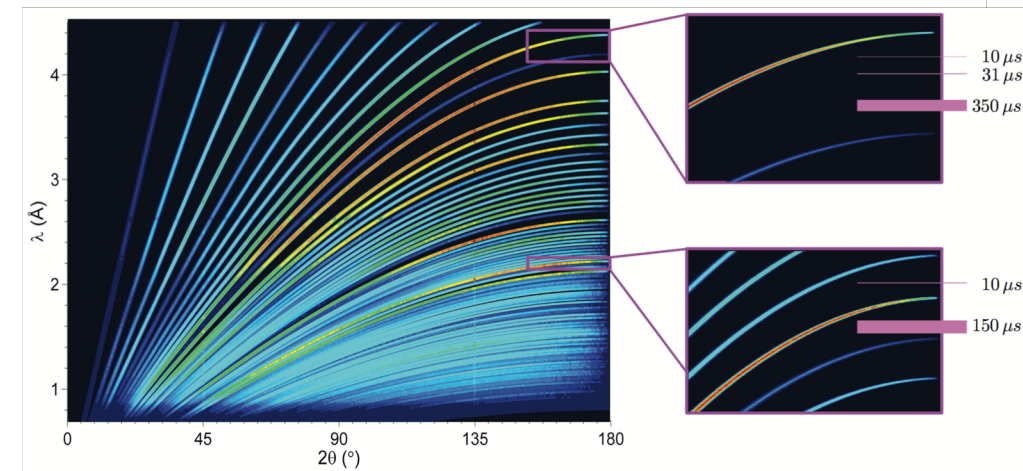
# Concepts and design – DREAM ESS Instrument design



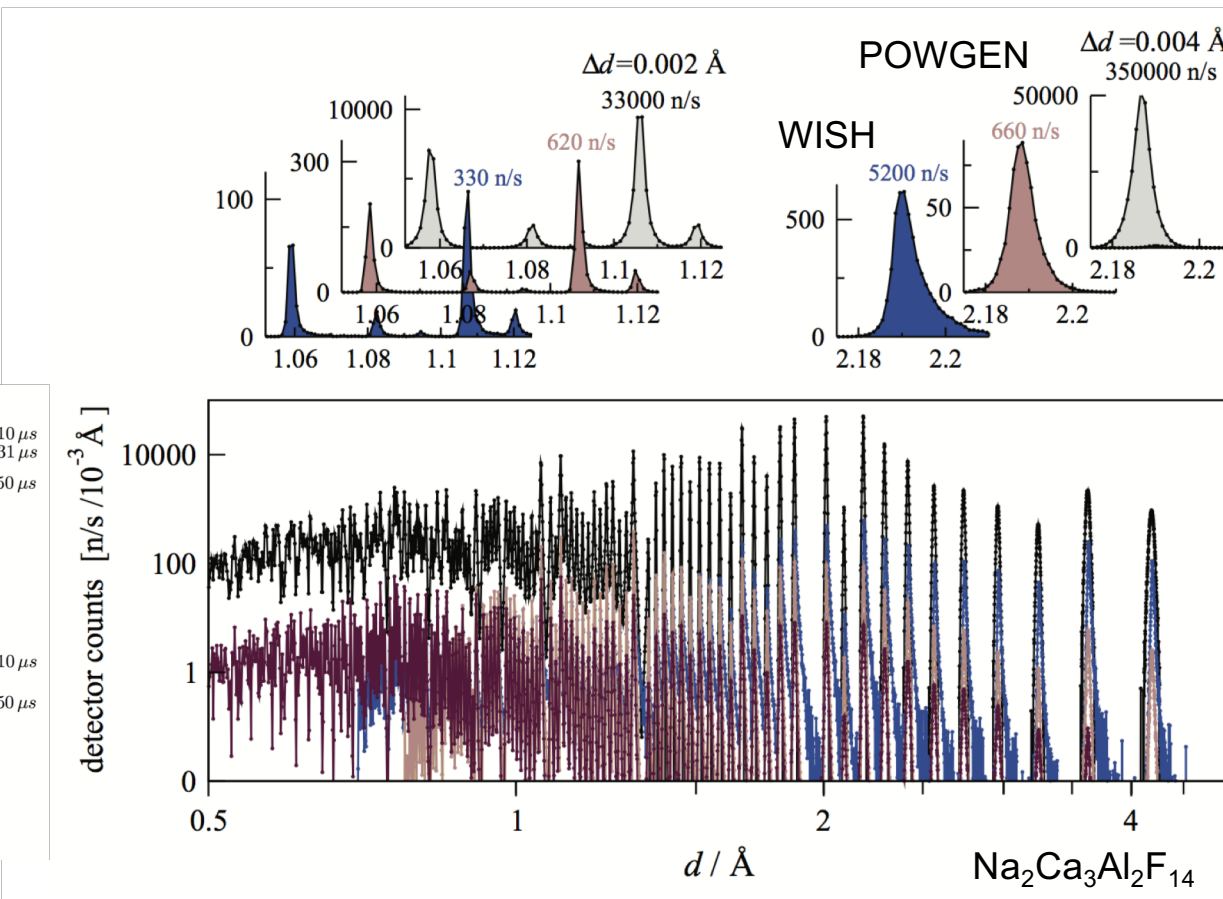
中国散裂中子源

# 2019 CSNS *McStas* *School*

McStas

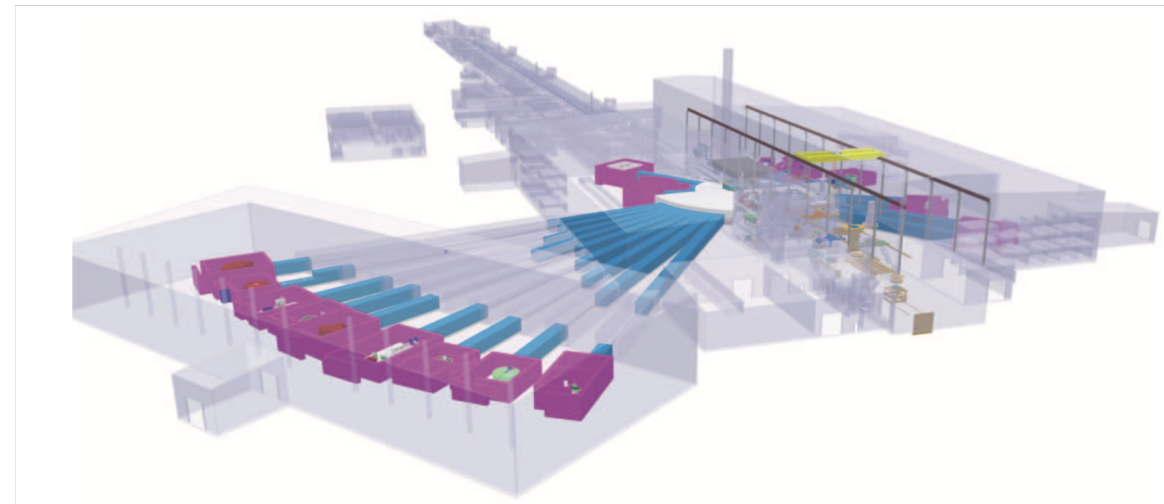


- Comparison to existing instrumentation
  - View of 2D data collection



W Schweika, N Violini, K Lieutenant, C Zendler, D Nekrassov, A Houben, P Jacobs and P F Henry

2016 J. Phys.: Conf. Ser. 746 012013



- Simulation of straw-man instrument suite for range of pulse time structures

TABLE I. Properties of 15 generic ESS instruments, suggested by the ESS-S SAG and the ESS SAC.  $L_1$  denotes the length of the instrument for a pulse length of  $\tau = 1$  ms, while  $L_2$  is the instrument length for  $\tau = 2$  ms, and  $\beta$  is the “Frascati exponent,” defined by (1).

Instrument	$L_1$ (m)	$L_2$ (m)	$\beta$
Cold chopper spect.	60	100	0
Therm. chopper spect.	100	100	0
Cold triple axis	40	40	0
Thermal triple axis	40	40	0
TOF triple axis	60	100	0
Backscatter spectrometer	151	302	0
Spin echo spectrometer	30	30	2.5
Short SANS (bio-)	12 + 1–4		2.5
Medium SANS	18 + 1–10		2.5
Long SANS (materials-)	28 + 2–20		2.5
Horizontal reflectometer	52	52	4
Vertical reflectometer	52	52	4
Cold powder diffract.	88	176	0
Thermal powder diffract.	102	102	0
Single crystal diffract.	31	42	0

Kim Lefmann, Kaspar H. Klenø, Jonas Okkels Birk, Britt R. Hansen, Sonja L. Holm, Erik Knudsen, Klaus Lieutenant, Lars von Moos, Morten Sales, Peter K. Willendrup, and Ken H. Andersen. Review of Scientific Instruments **84**, 055106 (2013); doi: 10.1063/1.4803167

# Global optimization – Generic ESS instrument suite

- Example: IN5-like cold chopper spectrometer

TABLE II. Relative Figure-of-Merit (FoM) values for the simulations of the IN5-like cold chopper spectrometer at ESS, under the assumption of constant time-average flux. Simulations are performed for 20 different settings of the time structure,  $(T, \tau)$ . The RRM scheme is parametrized by  $N$ , which indicates the number of possible monochromatic pulses at the sample per source pulse.

$T$ (ms)	$\tau$ (ms)	1.0	1.25	1.5	2.0	$N$
100 (10 Hz)		2.39	2.24	2.05	1.67	15
80 (12.5 Hz)		2.08	1.83	1.59	1.26	11
60 (16.67 Hz)		1.72	1.48	1.29	1.00	9
50 (20 Hz)		1.35	1.17	0.98	0.76	7
40 (25 Hz)		0.91	0.81	0.68	0.56	5

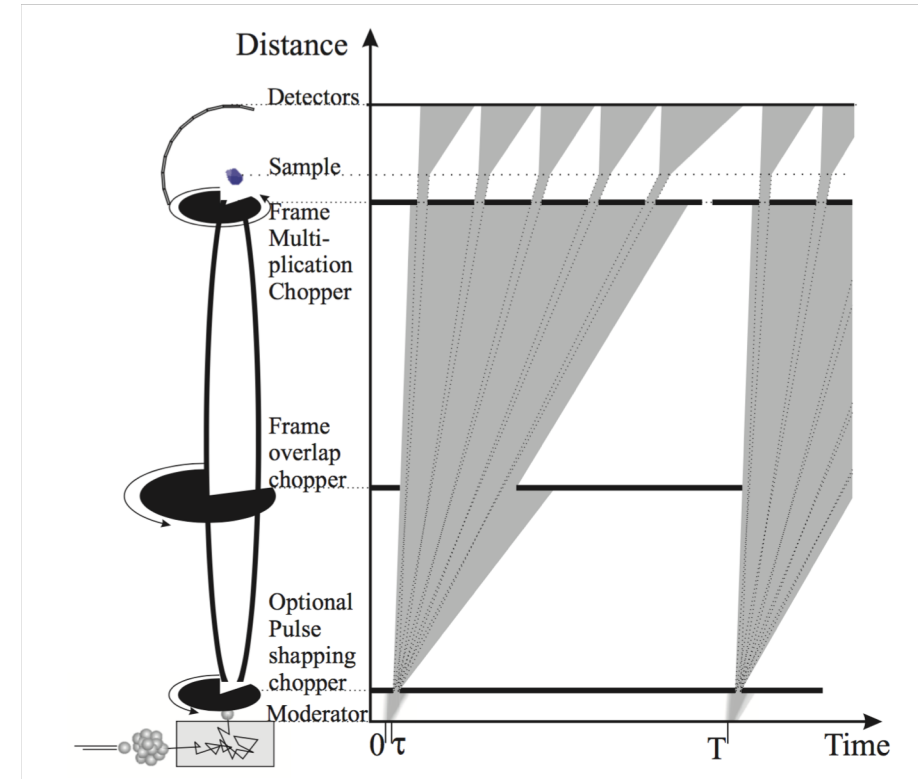


FIG. 2. (left) Sketch of the main elements of the cold chopper spectrometer. Picture is not to scale. (right) Time-of-flight diagram illustrating the selection of neutron pulses by choppers, with the spectrometer running in RRM mode with  $N = 5$ .

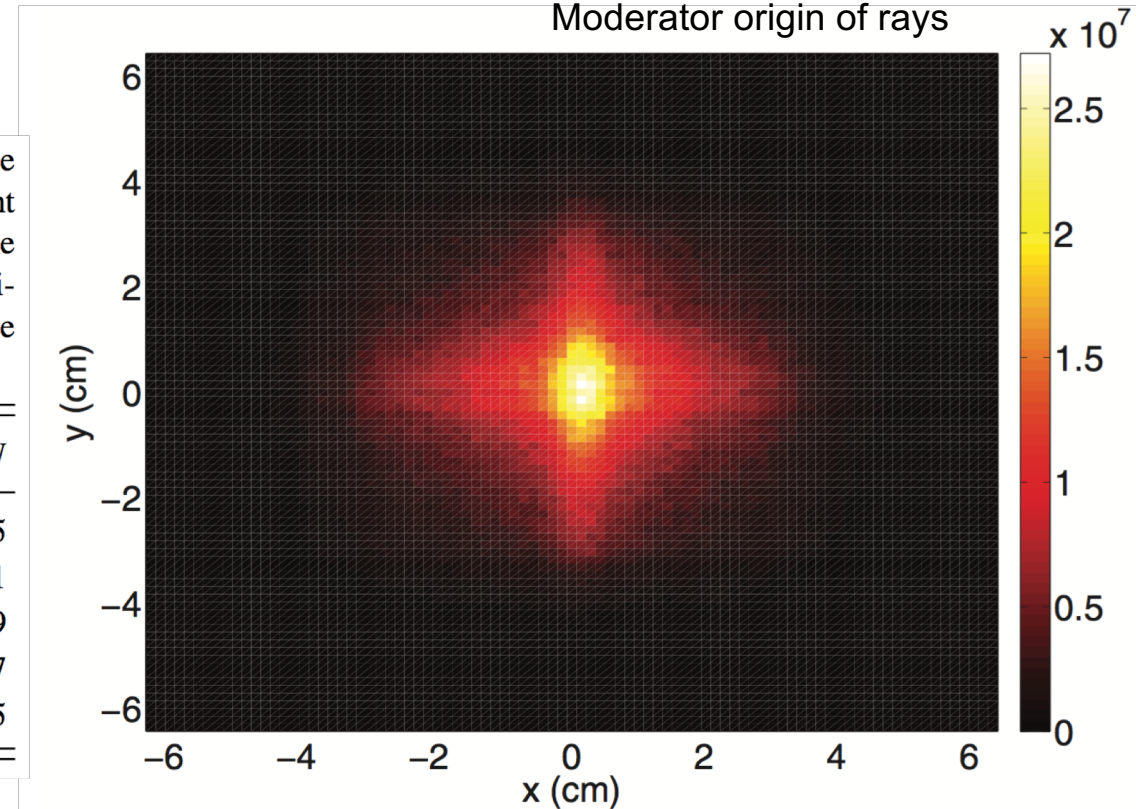
Kim Lefmann, Kaspar H. Klenø, Jonas Okkels Birk, Britt R. Hansen, Sonja L. Holm, Erik Knudsen, Klaus Lieutenant, Lars von Moos, Morten Sales, Peter K. Willendrup, and Ken H. Andersen. Review of Scientific Instruments **84**, 055106 (2013); doi: 10.1063/1.4803167

# Global optimization – Generic ESS instrument suite

- Example: IN5-like cold chopper spectrometer

TABLE II. Relative Figure-of-Merit (FoM) values for the simulations of the IN5-like cold chopper spectrometer at ESS, under the assumption of constant time-average flux. Simulations are performed for 20 different settings of the time structure,  $(T, \tau)$ . The RRM scheme is parametrized by  $N$ , which indicates the number of possible monochromatic pulses at the sample per source pulse.

$T$ (ms)	$\tau$ (ms)	1.0	1.25	1.5	2.0	$N$
100 (10 Hz)		2.39	2.24	2.05	1.67	15
80 (12.5 Hz)		2.08	1.83	1.59	1.26	11
60 (16.67 Hz)		1.72	1.48	1.29	1.00	9
50 (20 Hz)		1.35	1.17	0.98	0.76	7
40 (25 Hz)		0.91	0.81	0.68	0.56	5



Kim Lefmann, Kaspar H. Klenø, Jonas Okkels Birk, Britt R. Hansen, Sonja L. Holm, Erik Knudsen, Klaus Lieutenant, Lars von Moos, Morten Sales, Peter K. Willendrup, and Ken H. Andersen. Review of Scientific Instruments **84**, 055106 (2013); doi: 10.1063/1.4803167

# Global optimization – Generic ESS instrument suite

TABLE IV. Average relative Figure-of-Merit for the generic ESS instrument suite at different time structures, under the assumption of constant time-average flux.

$T$ (ms)	$\tau$ (ms)	1.0	1.25	1.5	2.0
100 (10 Hz)		2.07	1.81	1.67	1.37
80 (12.5 Hz)		1.89	1.66	1.55	1.19
60 (16.67 Hz)		1.62	1.42	1.24	1.00
50 (20 Hz)		1.53	1.27	1.09	0.88
40 (25 Hz)		1.20	1.05	0.90	0.73

TABLE V. Average relative Figure-of-Merit for the generic ESS instrument suite at different time structures, under the assumption of constant peak flux.

$T$ (ms)	$\tau$ (ms)	1.0	1.25	1.5	2.0
100 (10 Hz)		0.62	0.68	0.75	0.82
80 (12.5 Hz)		0.71	0.78	0.87	0.89
60 (16.67 Hz)		0.81	0.89	0.93	1.00
50 (20 Hz)		0.92	0.95	0.98	1.05
40 (25 Hz)		0.90	0.98	1.01	1.09

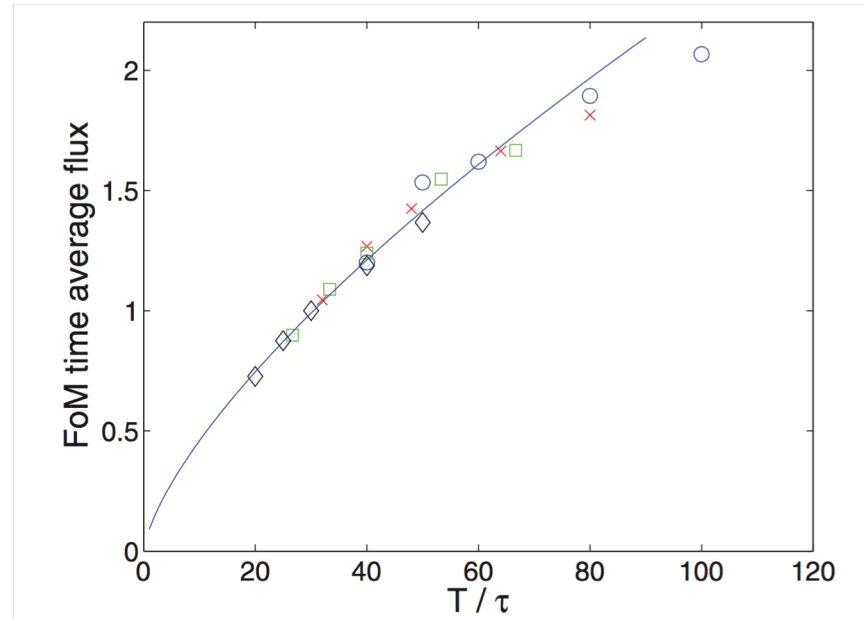


FIG. 6. Average Figure-of-Merit for the generic ESS instrument suite at different time structures, plotted as a function of the inverse source duty cycle, under the assumption of constant time-average flux. Diamonds, squares, crosses, and circles represent pulse lengths of 2.0, 1.5, 1.25, and 1.0 ms, respectively. The solid line is a fit to the power law (6), as explained in the text.

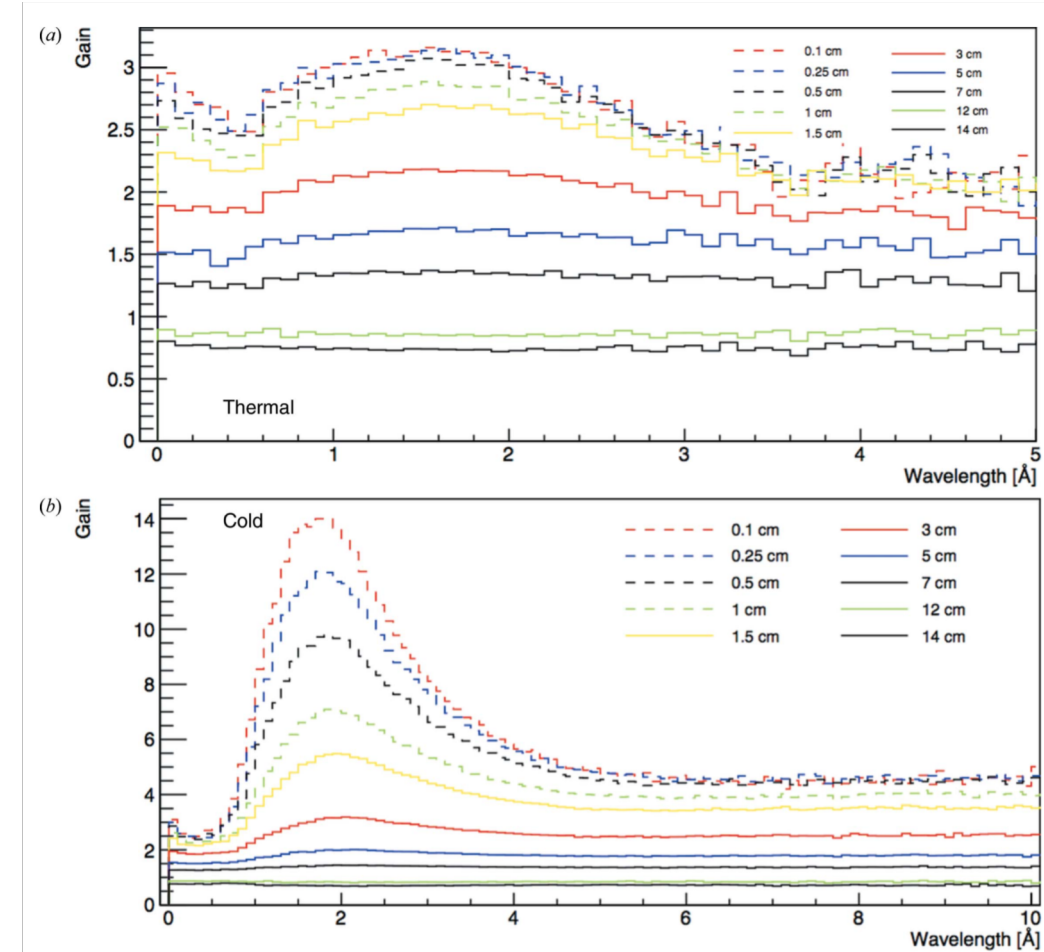
$$\text{FoM} \approx \Psi_{\text{peak}} \left( \frac{\tau}{T} \right)^{\alpha} = \Psi_{\text{peak}}^{1-\alpha} \Psi_{\text{time av}}^{\alpha} = \Psi_{\text{time av}} \left( \frac{T}{\tau} \right)^{1-\alpha}$$

Kim Lefmann, Kaspar H. Klenø, Jonas Okkels Birk, Britt R. Hansen, Sonja L. Holm, Erik Knudsen, Klaus Lieutenant, Lars von Moos, Morten Sales, Peter K. Willendrup, and Ken H. Andersen. Review of Scientific Instruments **84**, 055106 (2013); doi: 10.1063/1.4803167

Andersen, K. H., Bertelsen, M., Zanini, L., Klinkby, E. B., Schonfeldt, T.,  
 Bentley, P. M., & Saroun, J. (2018). Journal of Applied Crystallography, 51, 264-281.

# Global optimization – ESS Moderator optimization

- Brilliance gain from small moderator heights discovered by ESS target group
- Need to reconsider moderator

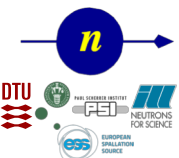


# Global optimization – ESS Moderator optimization

- Brilliance gain from small moderator heights discovered by ESS target group
- Need to reconsider moderator
- Guide optimization for range of moderator heights

2019 CSNS  
**McStas**  
**School**

**McStas**



Andersen, K. H., Bertelsen, M., Zanini, L., Klinkby, E. B., Schonfeldt, T.,  
Bentley, P. M., & Saroun, J. (2018). Journal of Applied Crystallography, 51, 264-281.

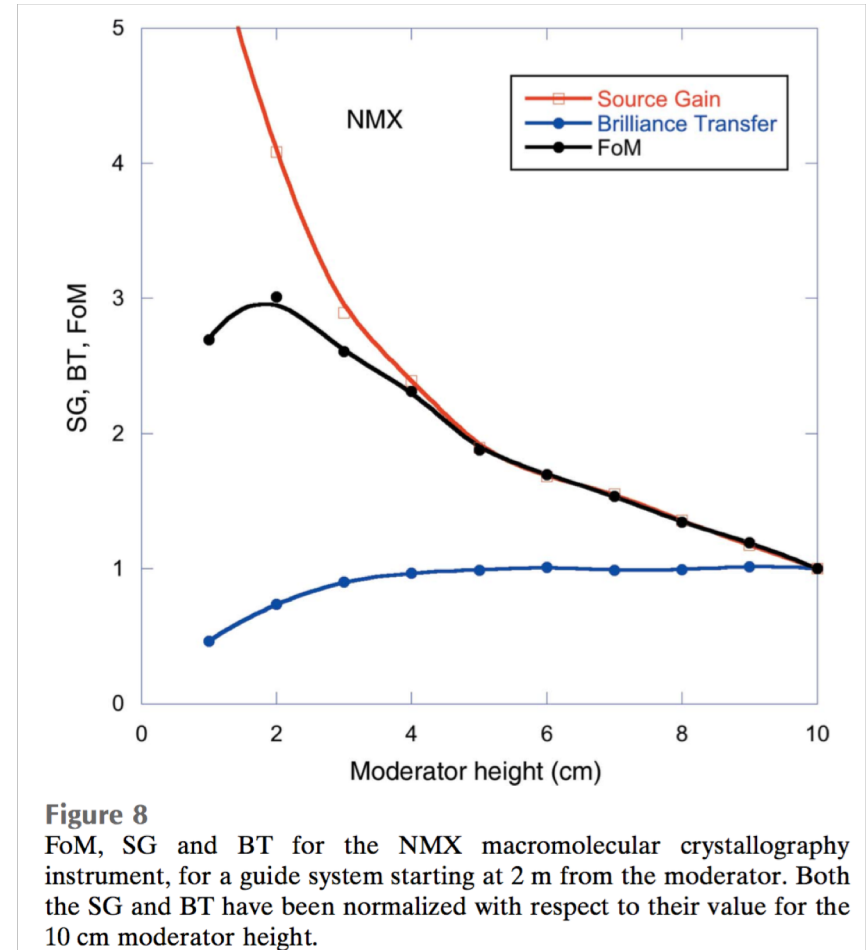


Figure 8

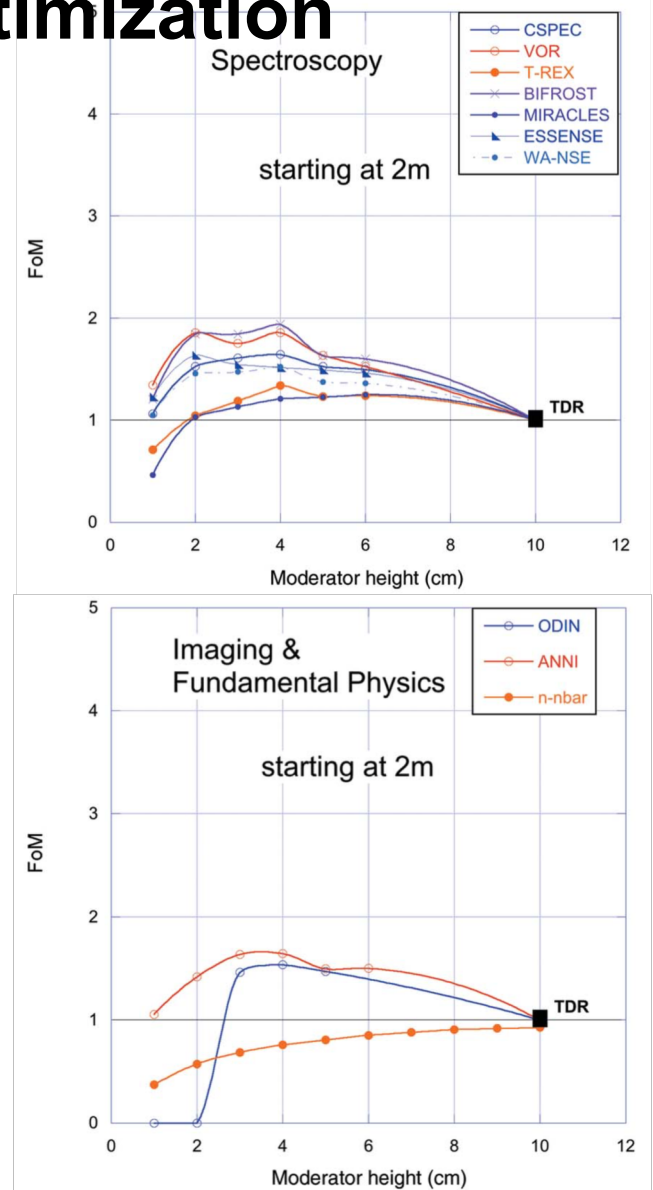
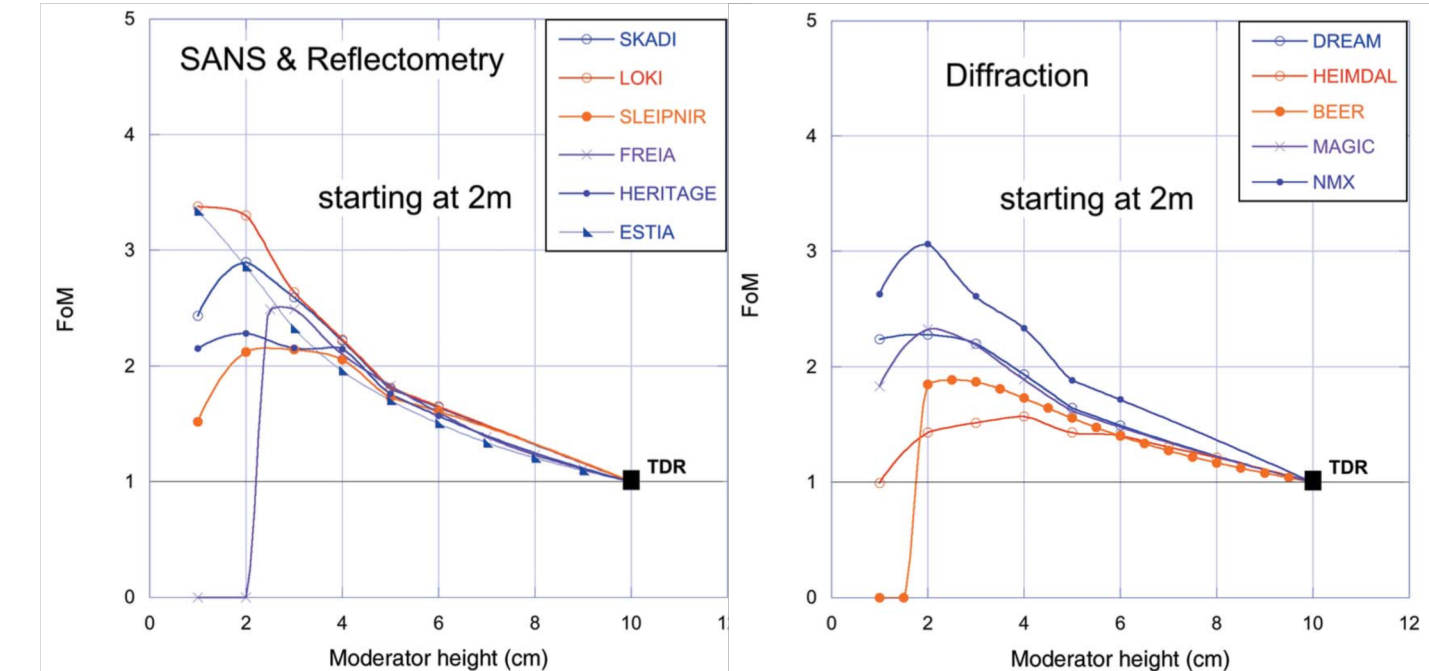
FoM, SG and BT for the NMX macromolecular crystallography instrument, for a guide system starting at 2 m from the moderator. Both the SG and BT have been normalized with respect to their value for the 10 cm moderator height.

# Global optimization – ESS Moderator optimization

Instrument	$L_{m-s}$	Beam area at sample (H × V)	Beam divergence at sample (H × V)	Wavelength range
Multi-purpose imaging ODIN	50 m	3 × 3 cm pinhole	At pinhole: $\pm 0.7 \times 0.7^\circ$	Bispectral, 1–7 Å
General-purpose polarized SANS SKADI	30 m	3 × 3 cm	$\pm 0.29 \times 0.29^\circ$	Cold, 2–10 Å
Broad-band high-flux SANS LOKI	20 m	3 × 3 cm	$\pm 0.57 \times 0.57^\circ$	Cold, 2–12 Å
Compact SANS SLEIPNIR*	16 m	2 × 2 cm	$\pm 0.86 \times 0.86^\circ$	Cold, 3–19 Å
Horizontal reflectometer FREIA	27 m	0.4 × 4 cm	$1.5 \times 4^\circ$	Cold, 2–9.5 Å
Alternative horizontal reflectometer HERITAGE*	36 m	1 × 1 cm	$\pm 2 \times 0.75^\circ$	Cold, 2–10 Å
Vertical reflectometer ESTIA	52 m	1 × 10 mm	$\pm 0.75 \times 0.75^\circ$	Cold, 5–9 Å
Pulsed monochromatic powder diffractometer HOD	$L_{m-m}$ 45 m	6 × 30 cm mono	At mono: $\pm 0.5 \times 0.5^\circ$	Thermal, 1.89 Å
Bispectral powder diffractometer DREAM	75 m	1 × 1 cm	$\pm 0.25 \times 0.25^\circ$	Bispectral, 0.8–4.6 Å
Hybrid diffractometer HEIMDAL*	167 m	5 × 15 mm	$\pm 0.24 \times 1.0^\circ$ $\pm 0.5 \times 0.5^\circ$	0.6–2.3 Å 4–10 Å
Materials science and engineering diffractometer BEER	157 m	5 × 10 mm	$\pm 0.14 \times 0.86^\circ$	Bispectral, 0.5–3.8 Å
Single-crystal magnetism diffractometer MAGIC	150 m	1 × 1 cm	$\pm 0.2 \times 0.2^\circ$ $\pm 0.5 \times 0.5^\circ$	0.7–2.4 Å 2.4–8 Å
Macromolecular diffractometer NMX	150 m	5 × 5 mm	$\pm 0.2 \times 0.2^\circ$	Cold, 1.5–3.3 Å
Cold chopper spectrometer CSPEC	151 m	1.9 × 4 cm	$\pm 1 \times 1^\circ$	Cold, 2–6 Å
Bispectral chopper spectrometer VOR	31 m	1 × 1 cm	$\pm 1 \times 1^\circ$	Cold, 1–9 Å
Alternative bispectral chopper spectrometer T-REX*	150 m	1 × 3 cm	$\pm 1 \times 1^\circ$	Bispectral, 0.8–7.2 Å
Thermal chopper spectrometer	160 m	3 × 3 cm	$\pm 1 \times 1^\circ$	Thermal, 0.6–3 Å
Cold crystal-analyser spectrometer BIFROST	170 m	15 × 15 mm	$\pm 0.75 \times 1^\circ$	Cold, 1.65–6.4 Å
Backscattering spectrometer MIRACLES	163 m	3 × 3 cm	$\pm 2.5 \times 2.5^\circ$	Cold, 2–8 Å
High-resolution spin echo ESSENSE	27 m + 4 m	3 × 3 cm	$\pm 0.57 \times 0.57^\circ$	Cold, 4–25 Å
Wide-angle spin echo WA-NSE	47 m + 4 m	1.5 × 6 cm	$\pm 0.5 \times 1^\circ$	Cold, 2–10 Å
Fundamental and particle physics ANNI	30 m	6 × 6 cm	$\pm 0.57 \times 0.57^\circ$	Cold, 3–8 Å
n-nbar beamline*	300 m	Moderator surface	Brightness × $\lambda^2$	Cold, 0–20 Å

Andersen, K. H., Bertelsen, M., Zanini, L., Klinkby, E. B., Schonfeldt, T.,

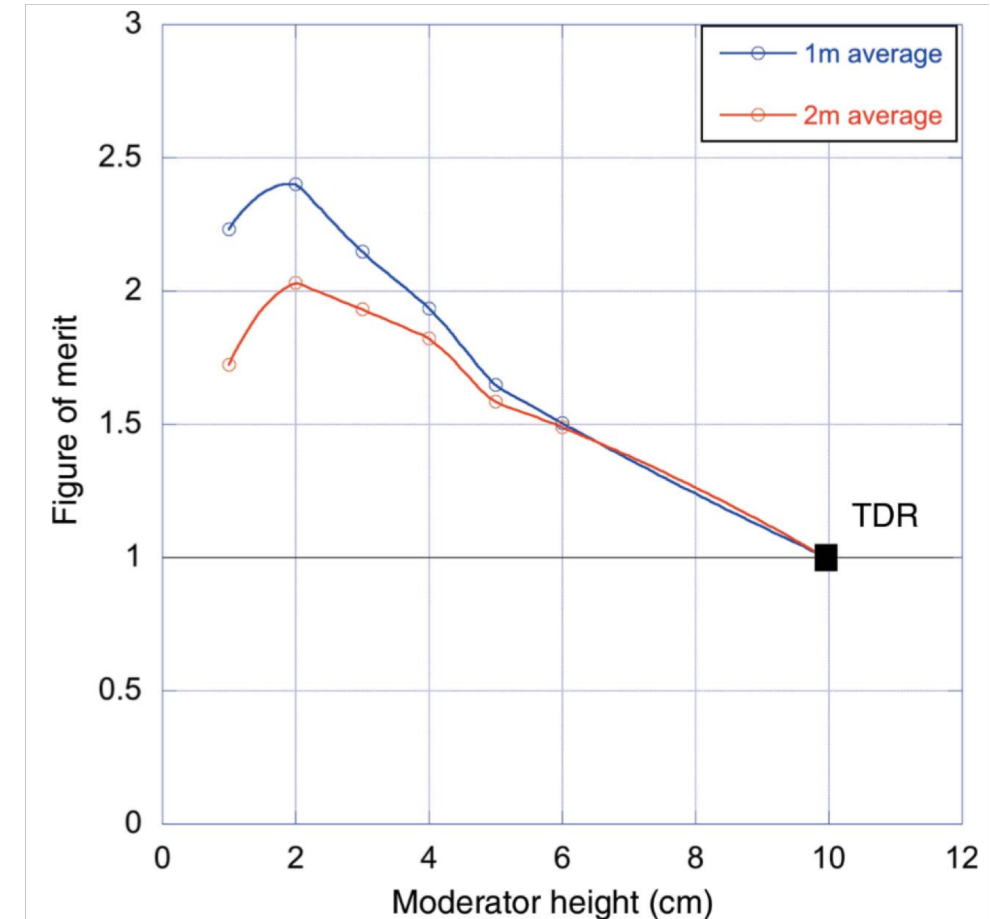
Bentley, P. M., & Saroun, J. (2018). Journal of Applied Crystallography, 51, 264-281.



Andersen, K. H., Bertelsen, M., Zanini, L., Klinkby, E. B., Schonfeldt, T.,  
Bentley, P. M., & Saroun, J. (2018). Journal of Applied Crystallography, 51, 264-281.

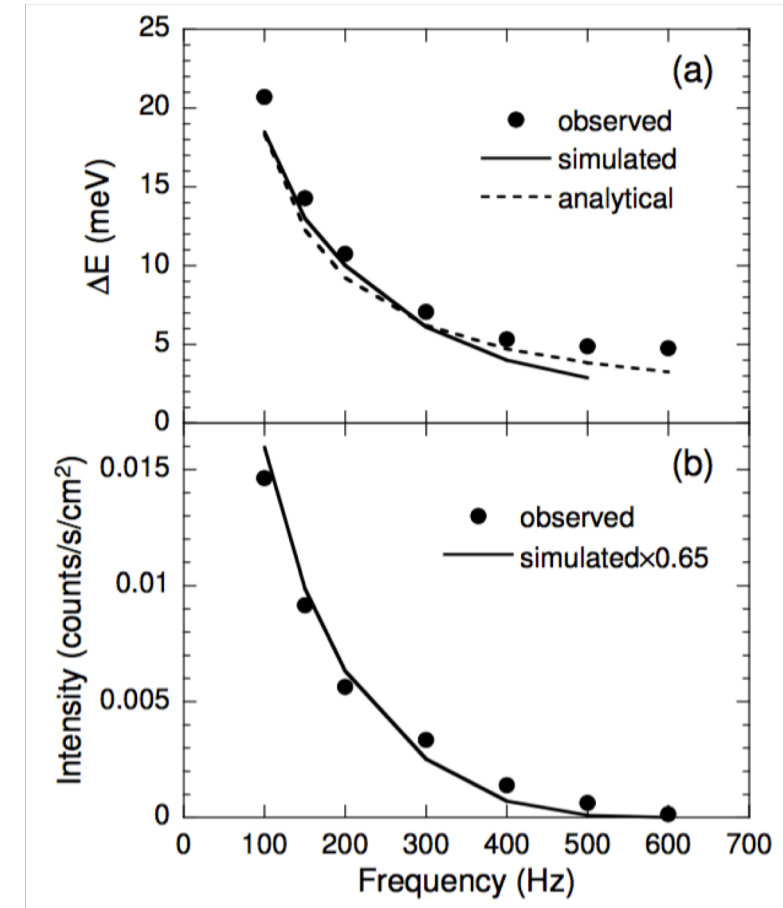
# Global optimization – ESS Moderator optimization

- Brilliance gain from small moderator heights discovered by ESS target group
- Need to reconsider moderator
- Guide optimization for range of moderator heights
- Sufficient data for informed decision



# Instrument papers – 4SEASONS @ J-PARC

- Resolution as expected in commissioning of 4SEASONS
- 65% of simulated intensity



## McStas

Ryoichi Kajimoto, Mitsutaka Nakamura, Yasuhiro Inamura, Fumio Mizuno, Kenji Nakajima, Seiko Ohira-Kawamura, Tetsuya Yokoo, Takeshi Nakatani,



Ryuji Maruyama, Kazuhiko Soyama, Kaoru Shibata, Kentaro Suzuya, Setsuo Sato, Kazuya Aizawa, Masatoshi Arai, Shuichi Wakimoto, Motoyuki Ishikado,



Shin-ichi Shamoto, Masaki Fujita, Haruhiro Hiraka, Kenji Ohoyama, Kazuyoshi Yamada, and Chul-Ho Lee. J. Phys. Soc. Jpn. **80** (2011) SB025

# Instrument papers – SEQUOIA @ SNS

- SEQUOIA Instrument paper
- Needed to adjust for:
  - Al windows
  - Air in beam
  - Monitor energy response
  - Electronic response time
- No arbitrary scaling factor

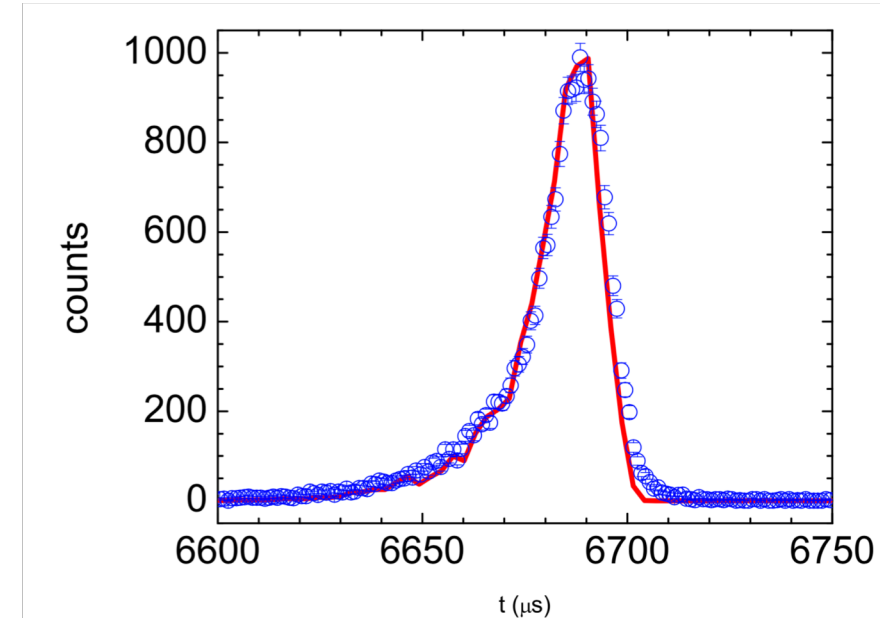


**Figure 2.** The signal observed in monitor 2 for  $E_i = 98$  meV neutrons. The solid line is the results of a Monte Carlo simulation of the instrument in the same conditions.

G. E. Granroth, A. I. Kolesnikov, T. E. Sherline, J. P. Clancy, K. A. Ross, J. P. C. Ruff, B. D. Gaulin, S. E. Nagler

2010 *J. Phys.: Conf. Ser.* **251** 012058

# Instrument papers – MACS @ NIST

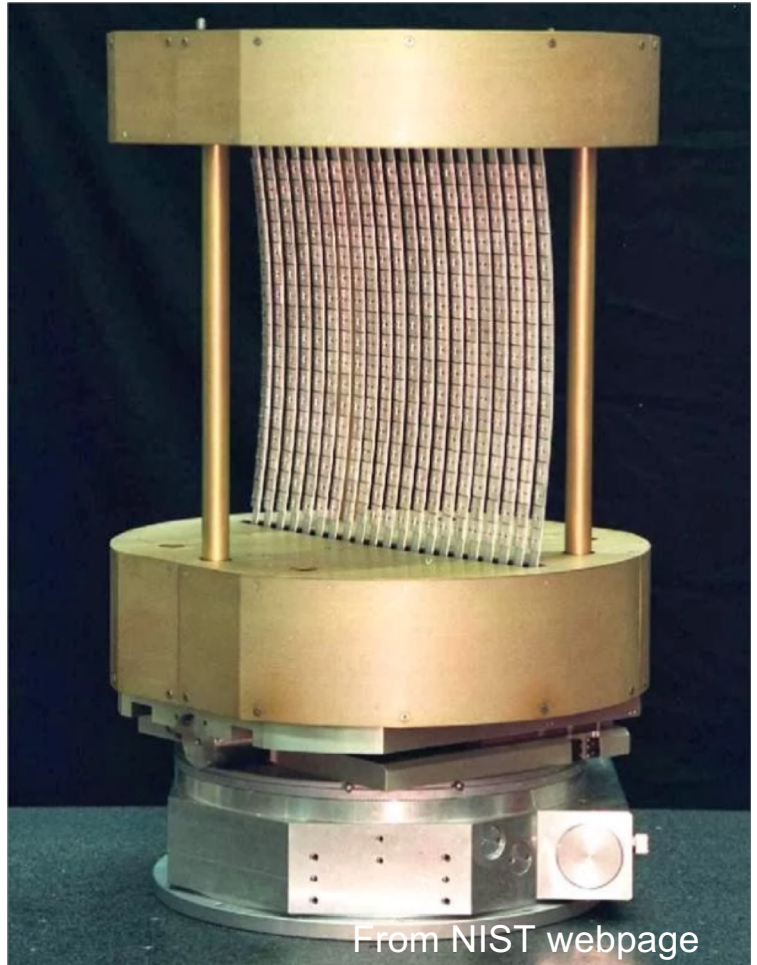
- MACS Monochromator characterization

$$L_0(2\theta) = L_0(2\theta = 90^\circ) - d_0/\tan 2\theta$$

$$L_1(2\theta) = d_1 + d_0/\sin 2\theta$$

$$R_v = \frac{2L_0 L_1 \sin \theta}{L_0 + L_1}$$

$$\tan \Psi_i = \frac{L_0}{L_0 \cot \xi - \rho_i / \sin \xi}$$



From NIST webpage

J A Rodriguez , D M Adler, P C Brand, C Broholm, J C Cook, C Brocker, R Hammond, Z Huang, P Hundertmark, J W Lynn,  
N C Maliszewskyj, J Moyer, J Orndorff, D Pierce, T D Pike, G Scharfstein, S A Smee and R Vilaseca. 2008 Meas. Sci. Technol. 19 034023

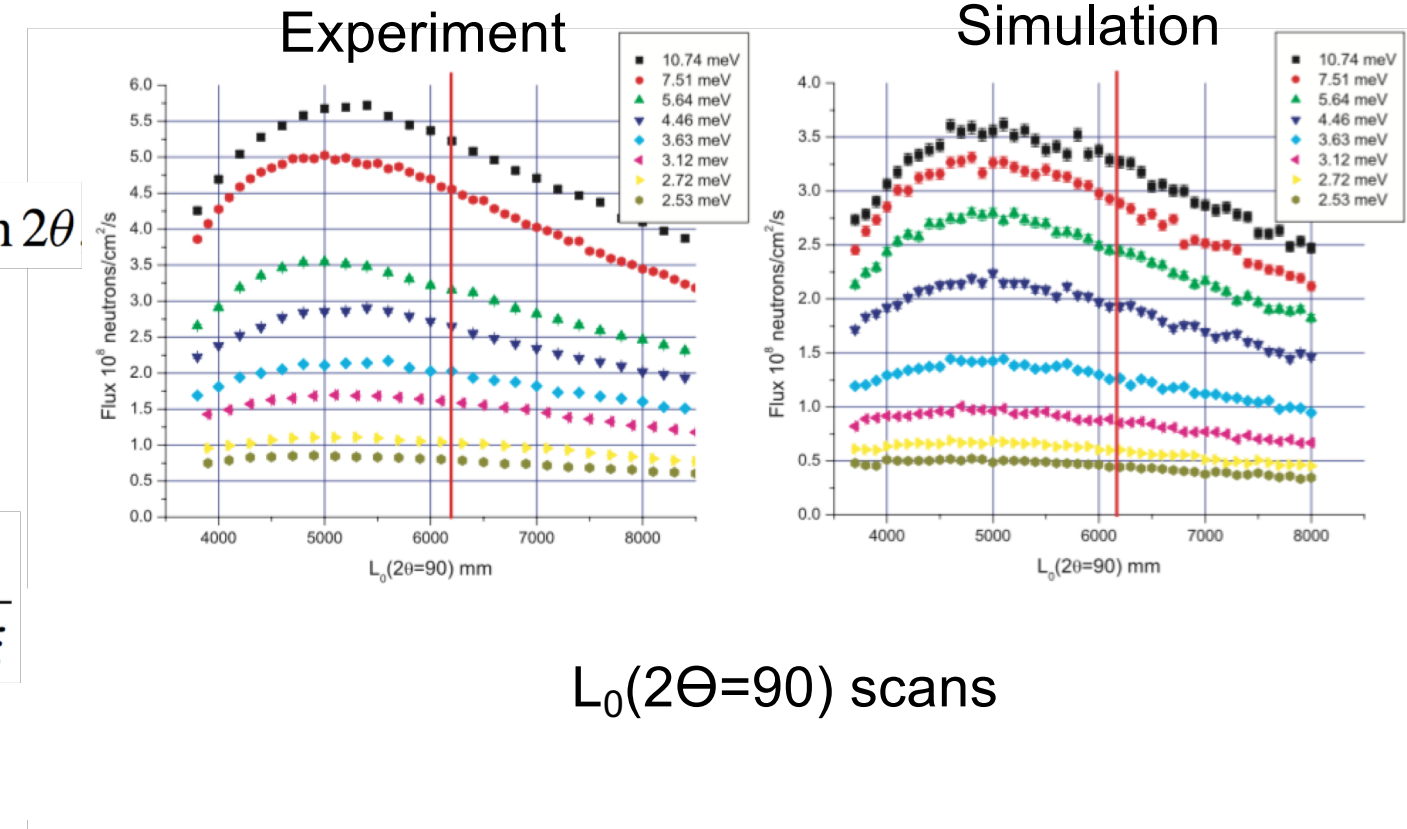
- MACS Monochromator characterization

$$L_0(2\theta) = L_0(2\theta = 90^\circ) - d_0/\tan 2\theta$$

$$L_1(2\theta) = d_1 + d_0/\sin 2\theta$$

$$R_v = \frac{2L_0 L_1 \sin \theta}{L_0 + L_1}$$

$$\tan \Psi_i = \frac{L_0}{L_0 \cot \xi - \rho_i / \sin \xi}$$



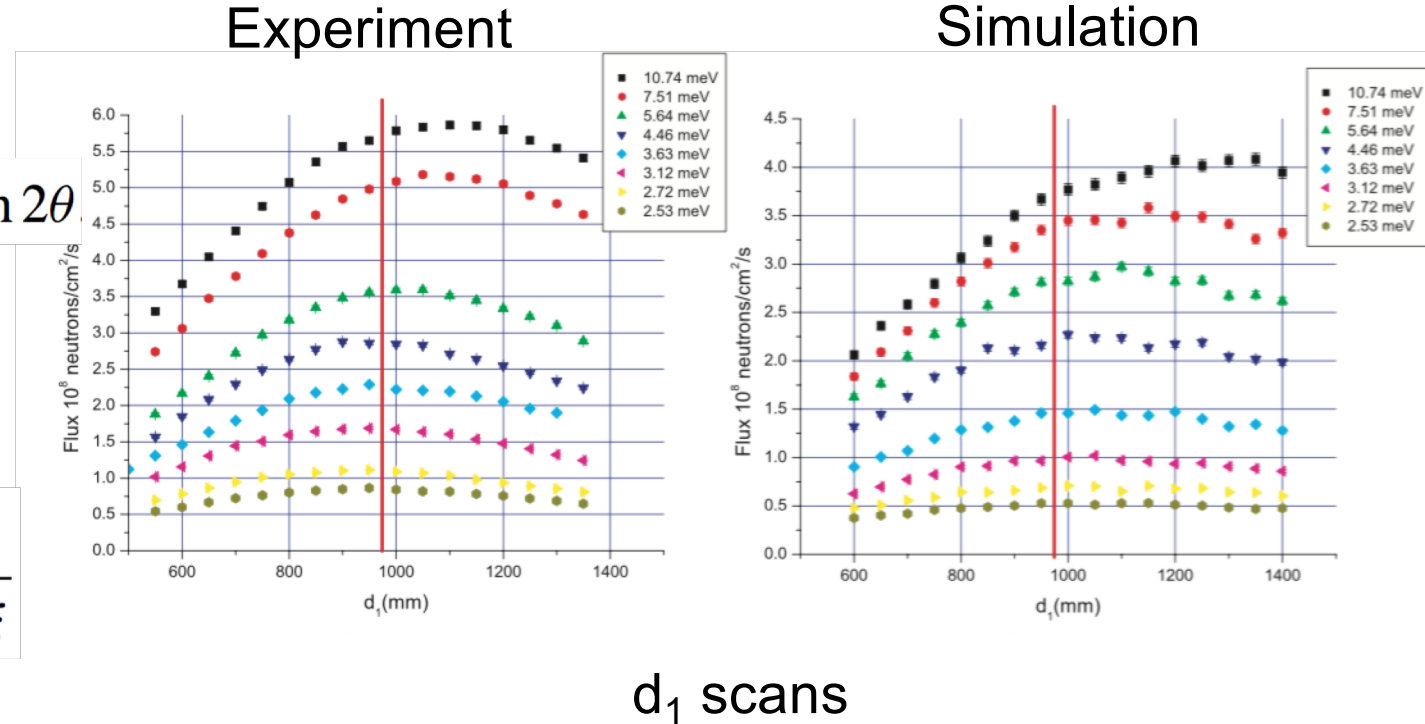
- MACS Monochromator characterization

$$L_0(2\theta) = L_0(2\theta = 90^\circ) - d_0/\tan 2\theta$$

$$L_1(2\theta) = d_1 + d_0/\sin 2\theta$$

$$R_v = \frac{2L_0 L_1 \sin \theta}{L_0 + L_1}$$

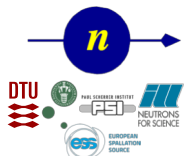
$$\tan \Psi_i = \frac{L_0}{L_0 \cot \xi - \rho_i / \sin \xi}$$



$d_1$  scans

2019 CSNS  
McStas  
School

McStas

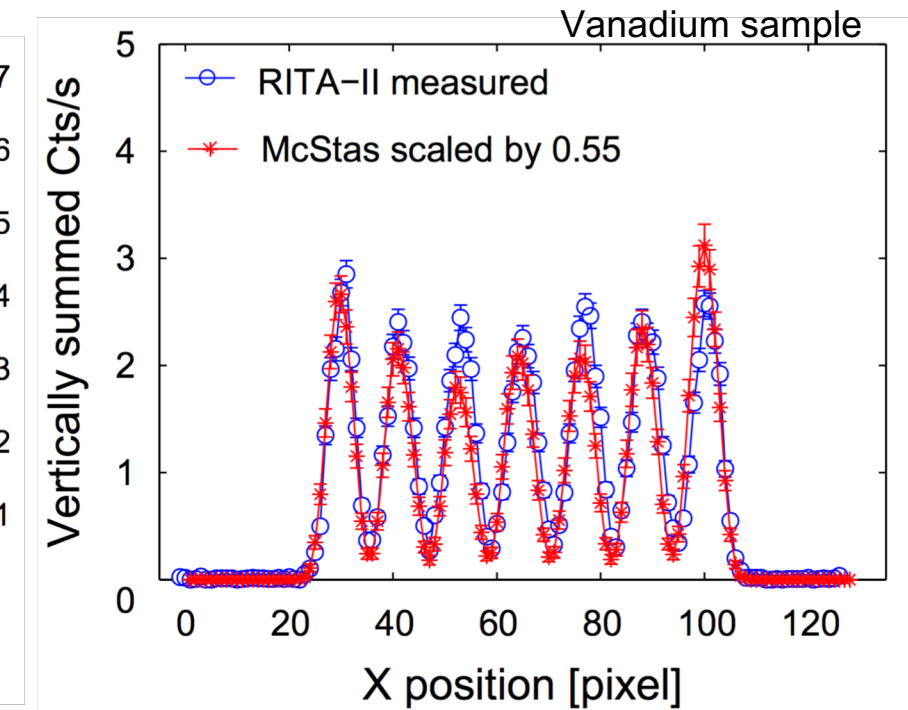
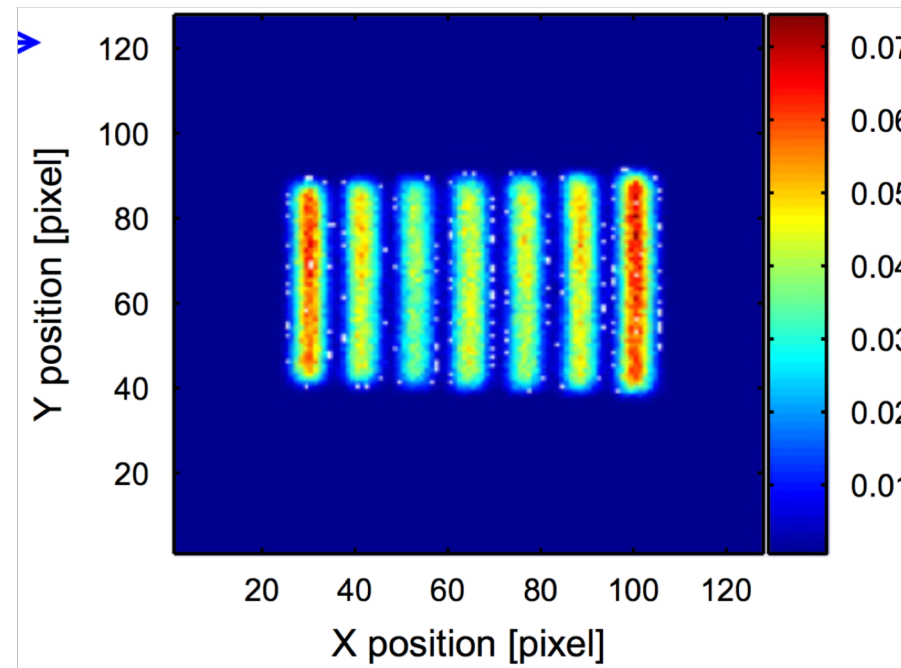


J A Rodriguez , D M Adler, P C Brand, C Broholm, J C Cook, C Brocker, R Hammond, Z Huang, P Hundertmark, J W Lynn,

N C Maliszewskyj, J Moyer, J Orndorff, D Pierce, T D Pike, G Scharfstein, S A Smee and R Vilaseca. 2008 Meas. Sci. Technol. 19 034023

# Virtual experiment benchmarks – RITAII @ PSI

- Triple axis spectrometer with 7 analyzer blades



L. Udby, P.K. Willendrup, E. Knudsen, Ch. Niedermayer, U. Filges, N.B. Christensen, E. Farhi, B.O. Wells, K. Lefmann.

Nuclear Instruments and Methods in Physics Research A 634 (2011) S138–S143

# Virtual experiment benchmarks – RITAII @ PSI

- Triple axis spectrometer with 7 analyzer blades
- Here measurement with center blade

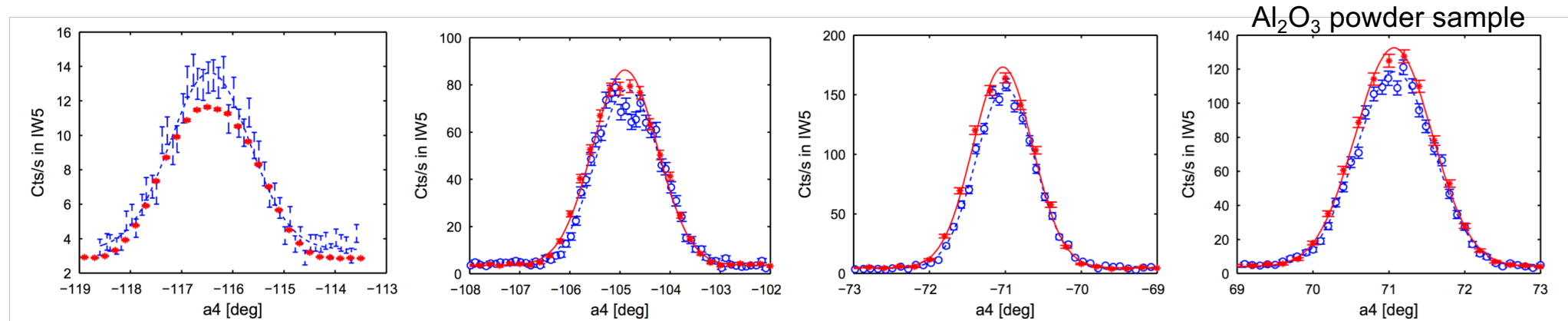


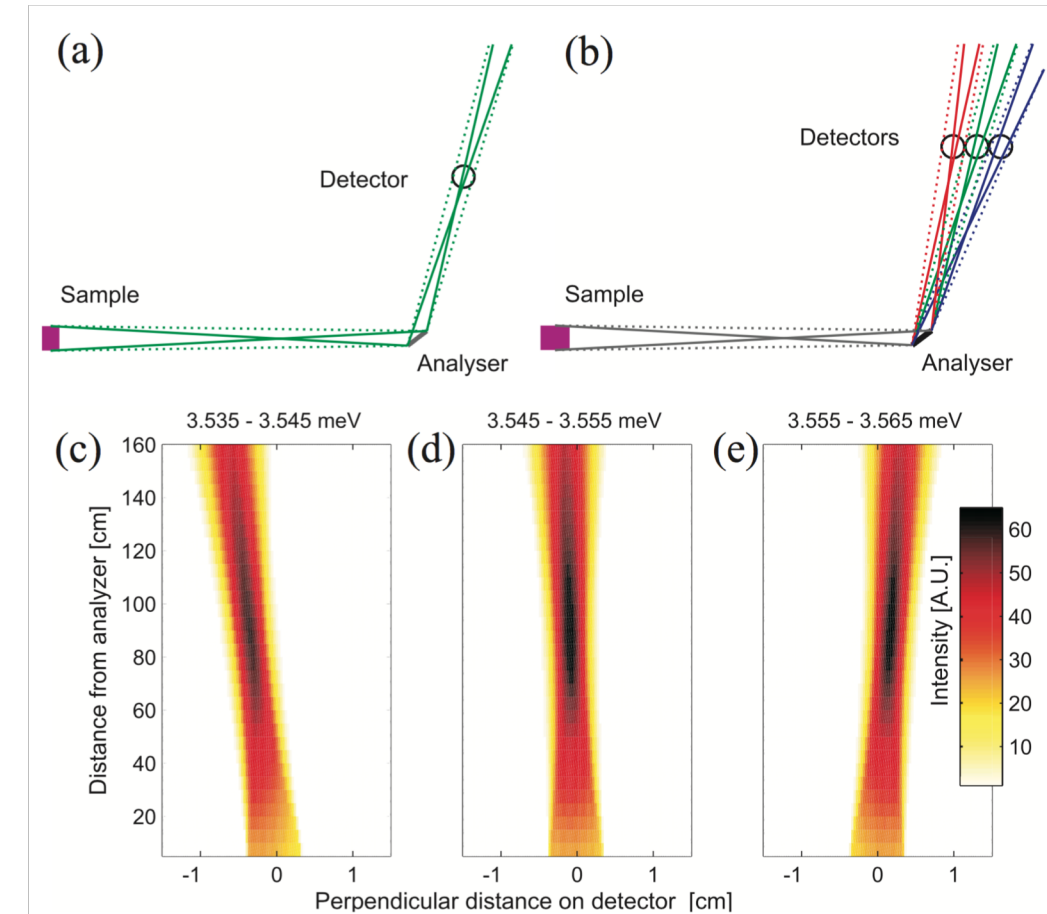
**Fig. 4.** Virtual (\*) and real (○) experimental data using a diffraction setup with focusing monochromator, 20' incoming collimation and an  $\text{Al}_2\text{O}_3$  powder sample. Figure (a) shows a scan across the (2 1 0) reflection cone, (b) the (1 0 4) reflection and (c) the (1 0 2) reflection all on the negative scattering side ( $a_4 < 0$ ). Figure (d) shows the (1 0 2) reflection on the positive scattering side ( $a_4 > 0$ ). Solid lines are fits to a simple Gaussian line shape.

L. Udby, P.K. Willendrup, E. Knudsen, Ch. Niedermayer, U. Filges, N.B. Christensen, E. Farhi, B.O. Wells, K. Lefmann.

Nuclear Instruments and Methods in Physics Research A 634 (2011) S138–S143

# Virtual experiment benchmarks – Prismatic analyzer

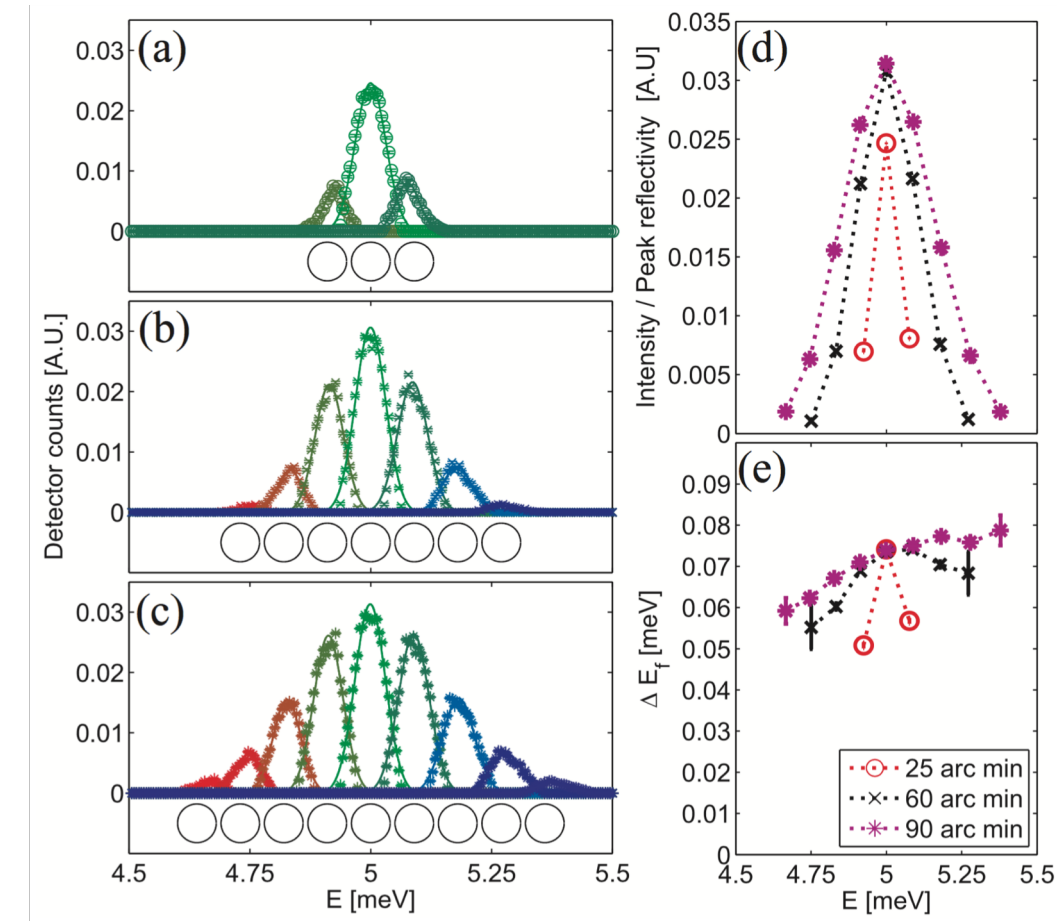
- Prismatic analyzer concept discovered under CAMEA / BIFROST development



Jonas O. Birk, Márton Markó, Paul G. Freeman, Johan Jacobsen, Rasmus L. Hansen, Niels B. Christensen, Christof Niedermayer, Martin Månnsson, Henrik M. Rønnow, and Kim Lefmann. Review of Scientific Instruments **85**, 113908 (2014); doi: 10.1063/1.4901160

# Virtual experiment benchmarks – Prismatic analyzer

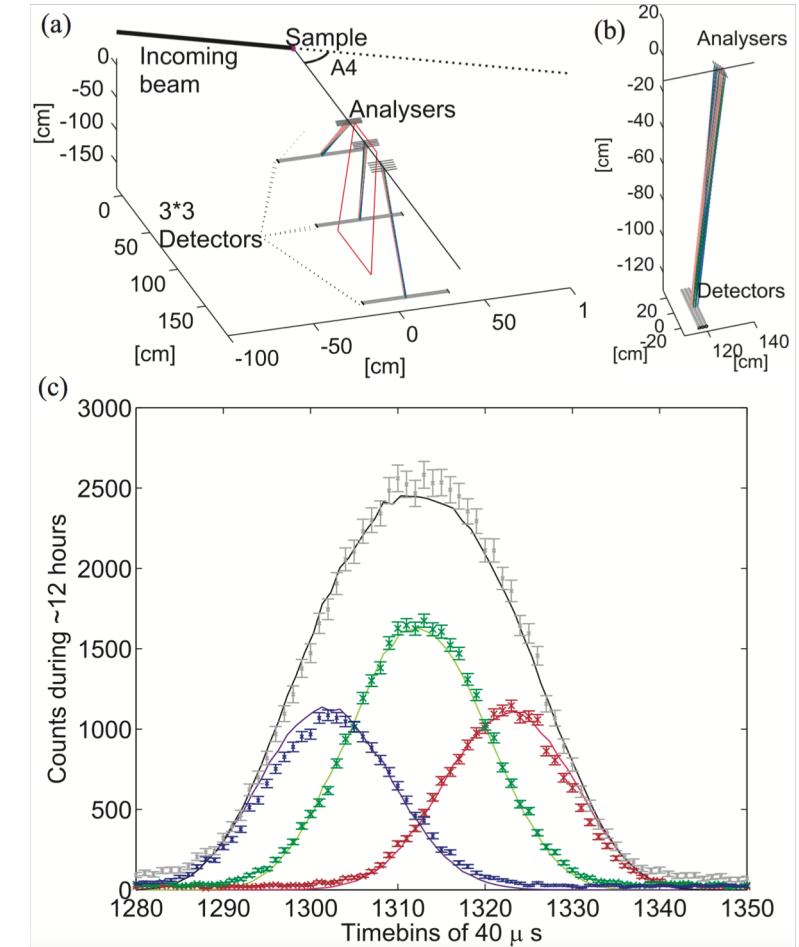
- Prismatic analyzer concept discovered under CAMEA / BIFROST development
- Simulations show it should work



Jonas O. Birk, Márton Markó, Paul G. Freeman, Johan Jacobsen, Rasmus L. Hansen, Niels B. Christensen, Christof Niedermayer, Martin Månsson, Henrik M. Rønnow, and Kim Lefmann. Review of Scientific Instruments **85**, 113908 (2014); doi: 10.1063/1.4901160

# Virtual experiment benchmarks – Prismatic analyzer

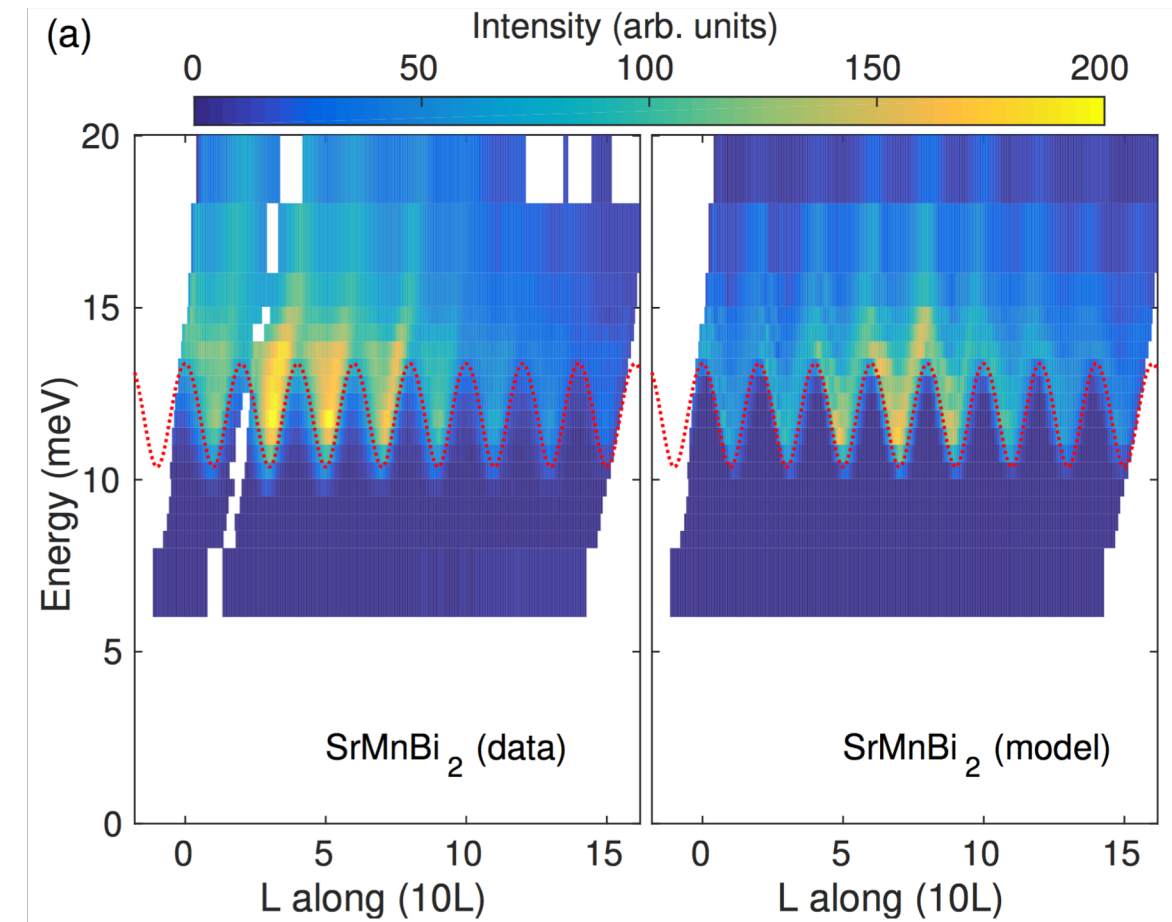
- Prismatic analyzer concept discovered under CAMEA / BIFROST development
- Simulations show it should work
- Measured on CAMEA prototype at PSI



Jonas O. Birk, Márton Markó, Paul G. Freeman, Johan Jacobsen, Rasmus L. Hansen, Niels B. Christensen, Christof Niedermayer, Martin Månsson, Henrik M. Rønnow, and Kim Lefmann. Review of Scientific Instruments **85**, 113908 (2014); doi: 10.1063/1.4901160

# Virtual experiment – Resolution convolution on IN8 @ ILL

- Dirac Metals
- Resolution convolution of fit with RESTRAX results



M. C. Rahn, A. J. Princep, A. Piovano, J. Kulda, Y. F. Guo, Y. G. Shi, and A. T. Boothroyd

Phys. Rev. B **95**, 134405 – Published 4 April 2017

# Virtual experiment – Resolution convolution on IN8 @ ILL

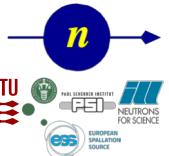


中  
國  
散  
裂  
中  
子  
源

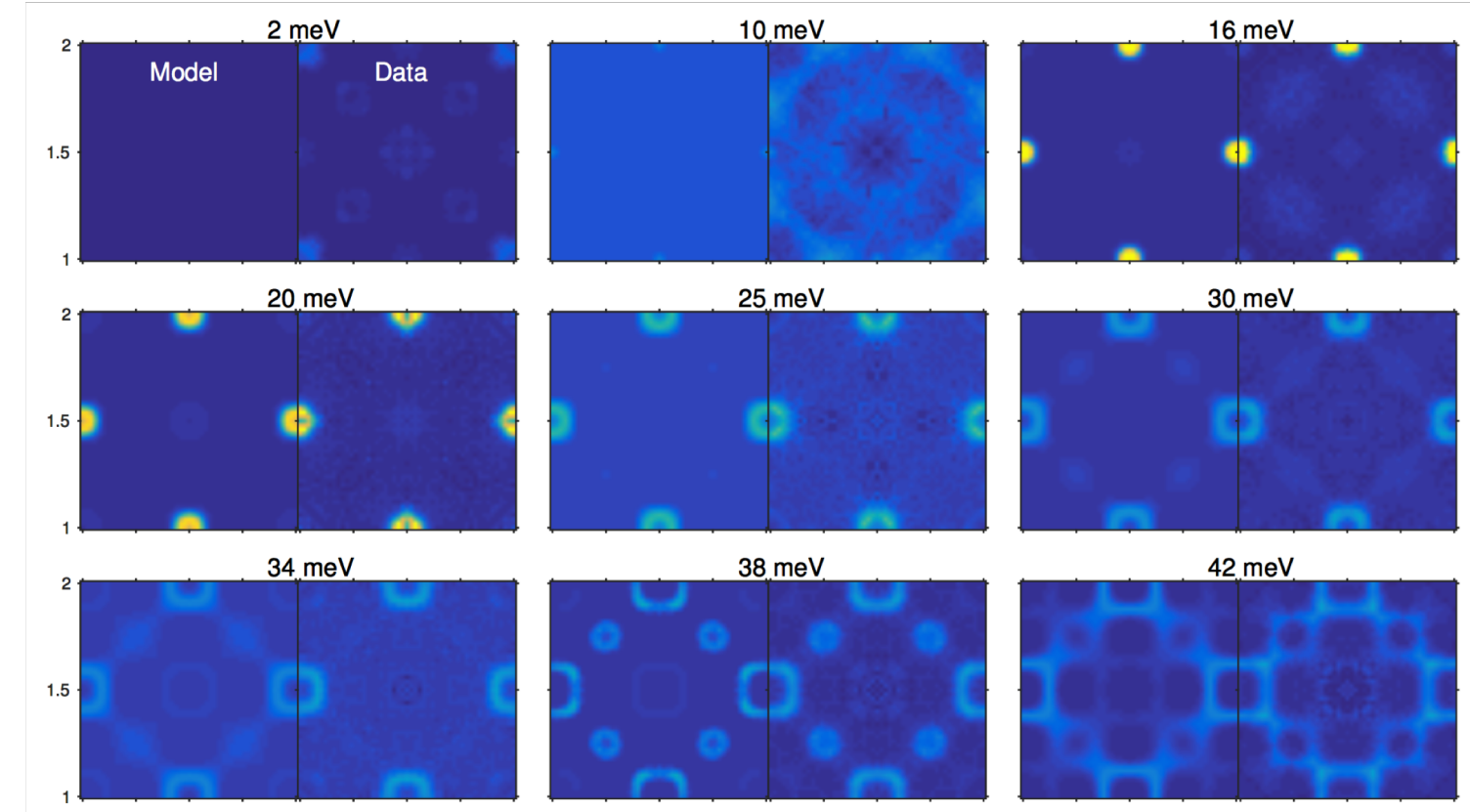
- Dirac Metals
- Convolved model compared with data

2019 CSNS  
*McStas*  
School

*McStas*



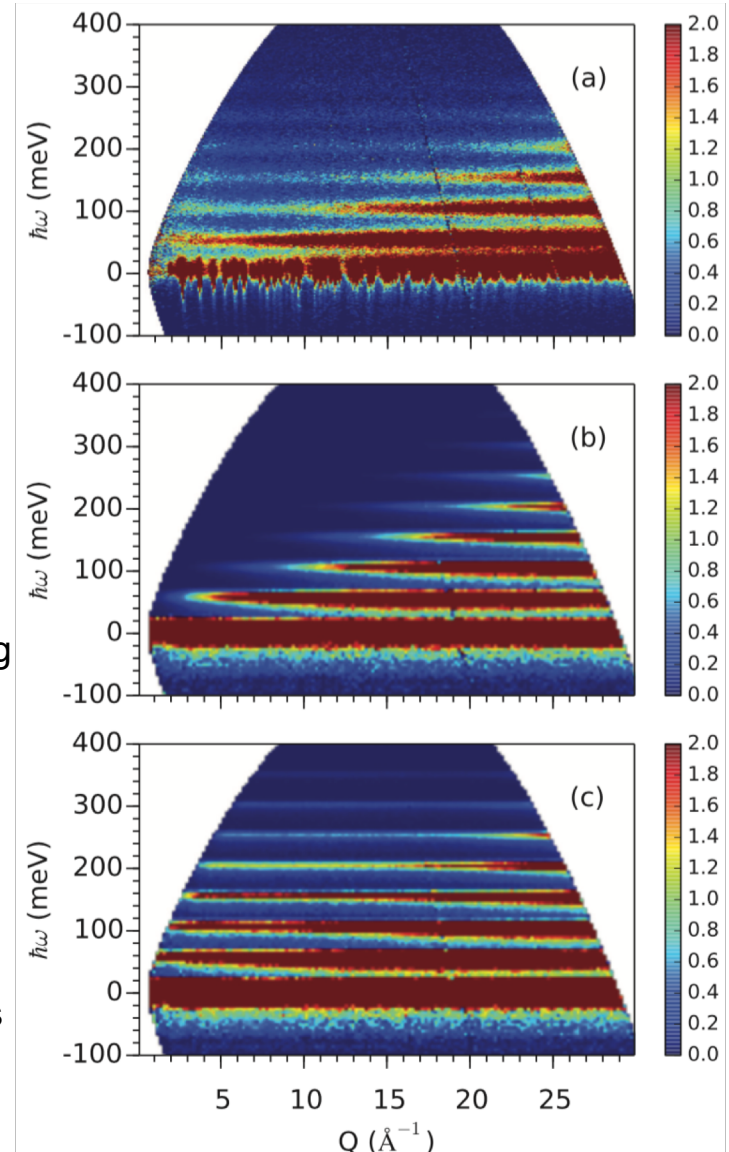
M. C. Rahn, A. J. Princep, A. Piovano, J. Kulda, Y. F. Guo, Y. G. Shi, and A. T. Boothroyd  
Phys. Rev. B 95, 134405 – Published 4 April 2017



# Virtual experiment – Uranium Nitride on ARCS and SEQUIOA @ SNS

- Uranium Nitride (MCViNE)
- Single / Multiple scattering

Experiment

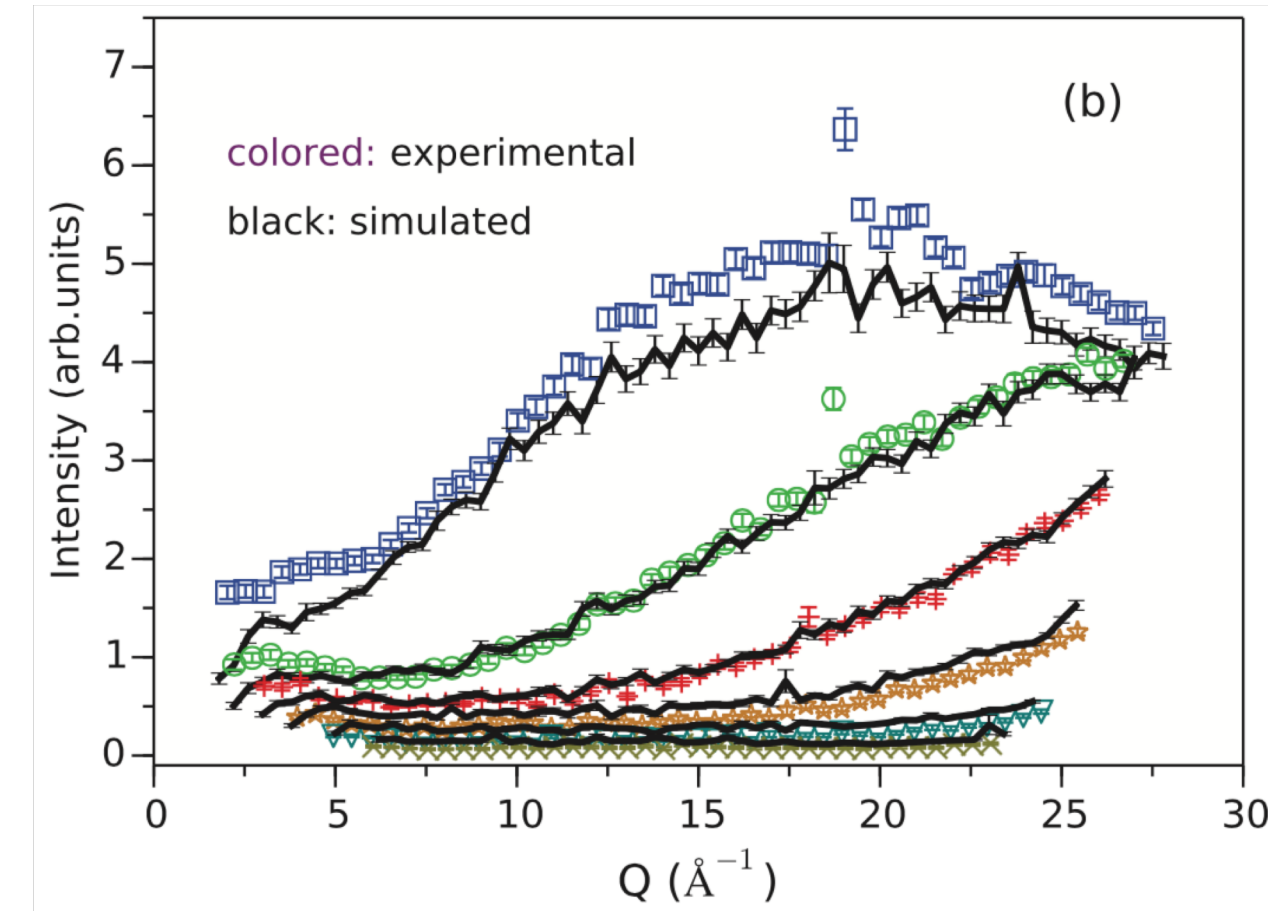
Simulated  
Single scatteringSimulated  
All scattering orders

J. Y. Y. Lin, A. A. Aczel, D. L. Abernathy, S. E. Nagler, W. J. L. Buyers, and G. E. Granroth

Phys. Rev. B **89**, 144302 – Published 7 April 2014

# Virtual experiment – Uranium Nitride on ARCS and SEQUIOA @ SNS

- Uranium Nitride (MCViNE)
- Single / Multiple scattering

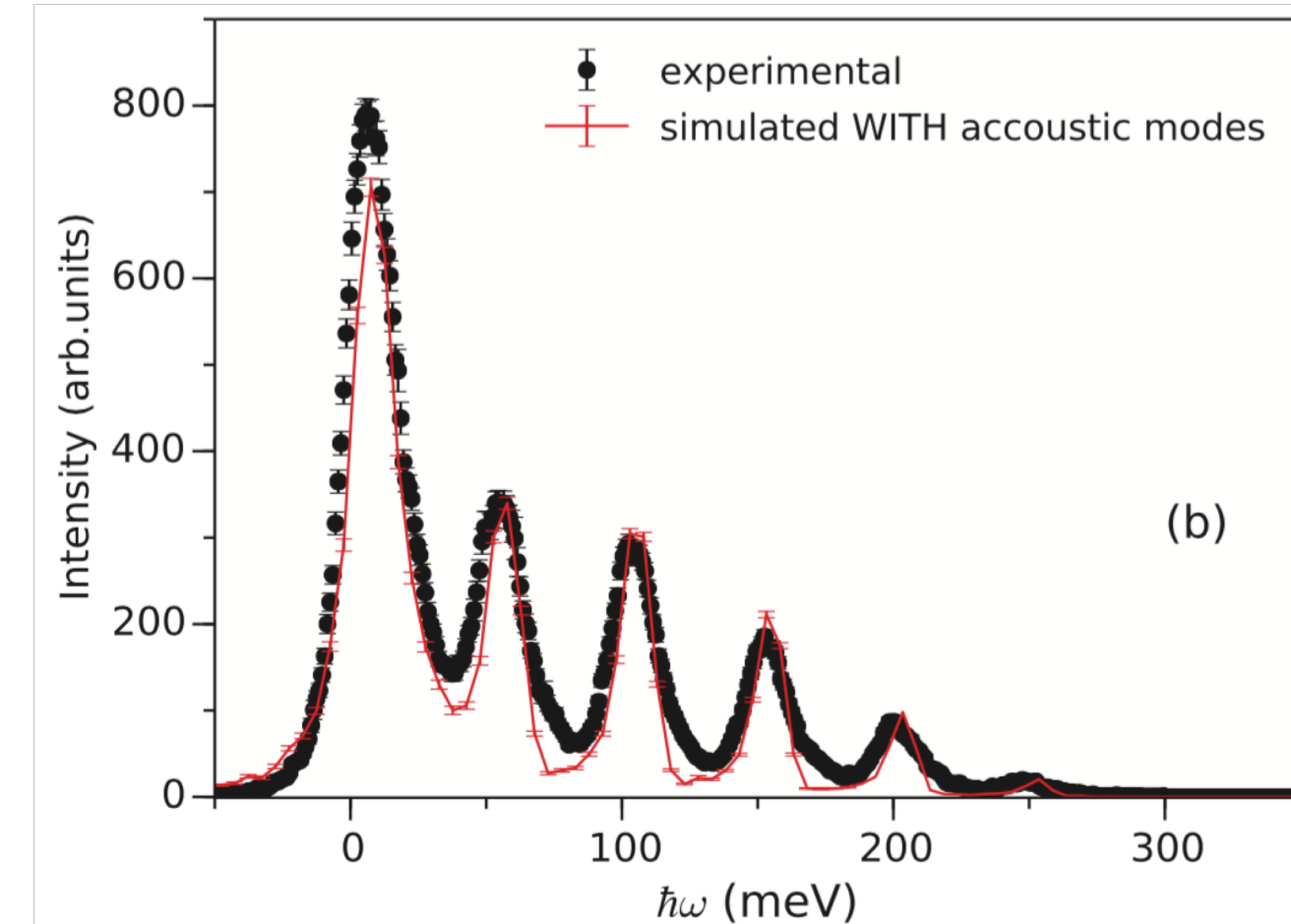


J. Y. Y. Lin, A. A. Aczel, D. L. Abernathy, S. E. Nagler, W. J. L. Buyers, and G. E. Granroth

Phys. Rev. B **89**, 144302 – Published 7 April 2014

# Virtual experiment – Uranium Nitride on ARCS and SEQUIOA @ SNS

- Uranium Nitride (MCViNE)
- Single / Multiple scattering



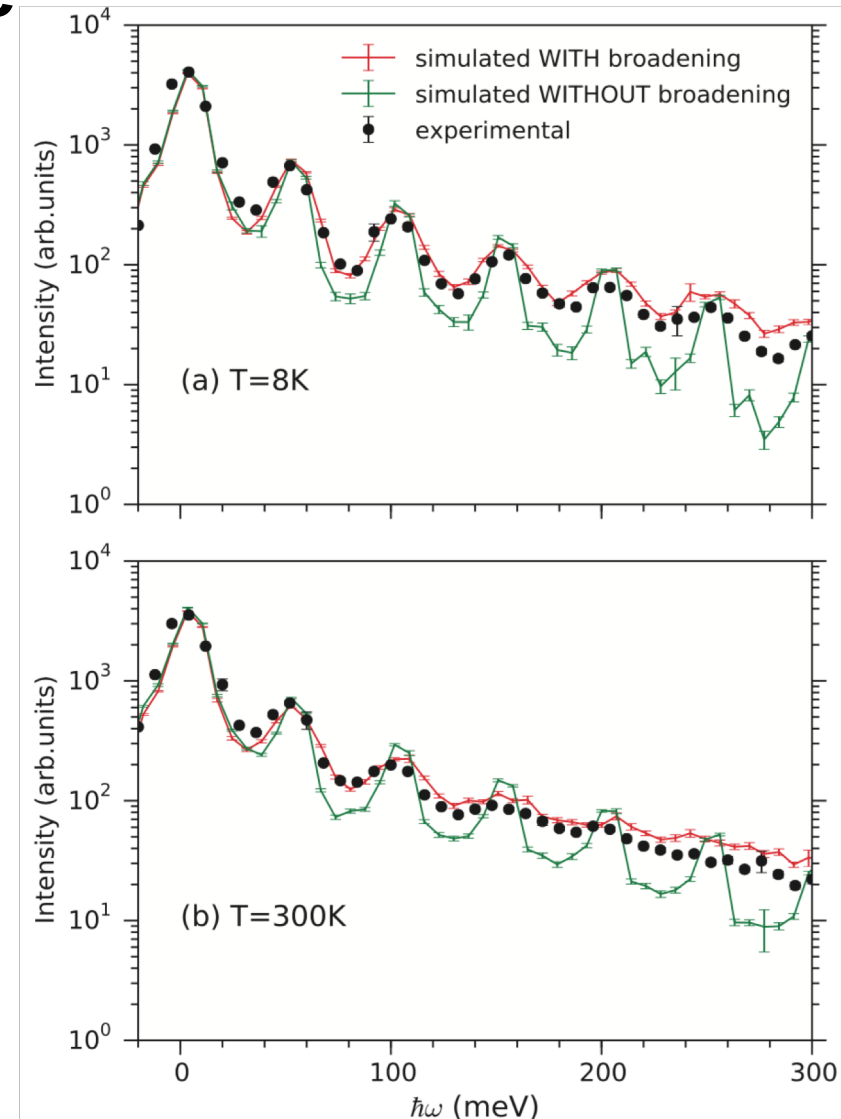
(b)

J. Y. Y. Lin, A. A. Aczel, D. L. Abernathy, S. E. Nagler, W. J. L. Buyers, and G. E. Granroth

Phys. Rev. B **89**, 144302 – Published 7 April 2014

# Virtual experiment – Uranium Nitride on ARCS and SEQUIOA @ SNS

- Uranium Nitride (MCViNE)
- Single / Multiple scattering
- Temperature broadening



J. Y. Y. Lin, A. A. Aczel, D. L. Abernathy, S. E. Nagler, W. J. L. Buyers, and G. E. Granroth

Phys. Rev. B **89**, 144302 – Published 7 April 2014

# Summary

- These packages are trusted
- Here we saw use in,
  - Facility level decisions
  - Instrument design
  - Benchmark for instrument test
  - Data analysis
- In addition to heavy use in optics
- Standard tool of the trade
- Expected continued growth
- Recent developments will encourage use in new areas

2019 CSNS

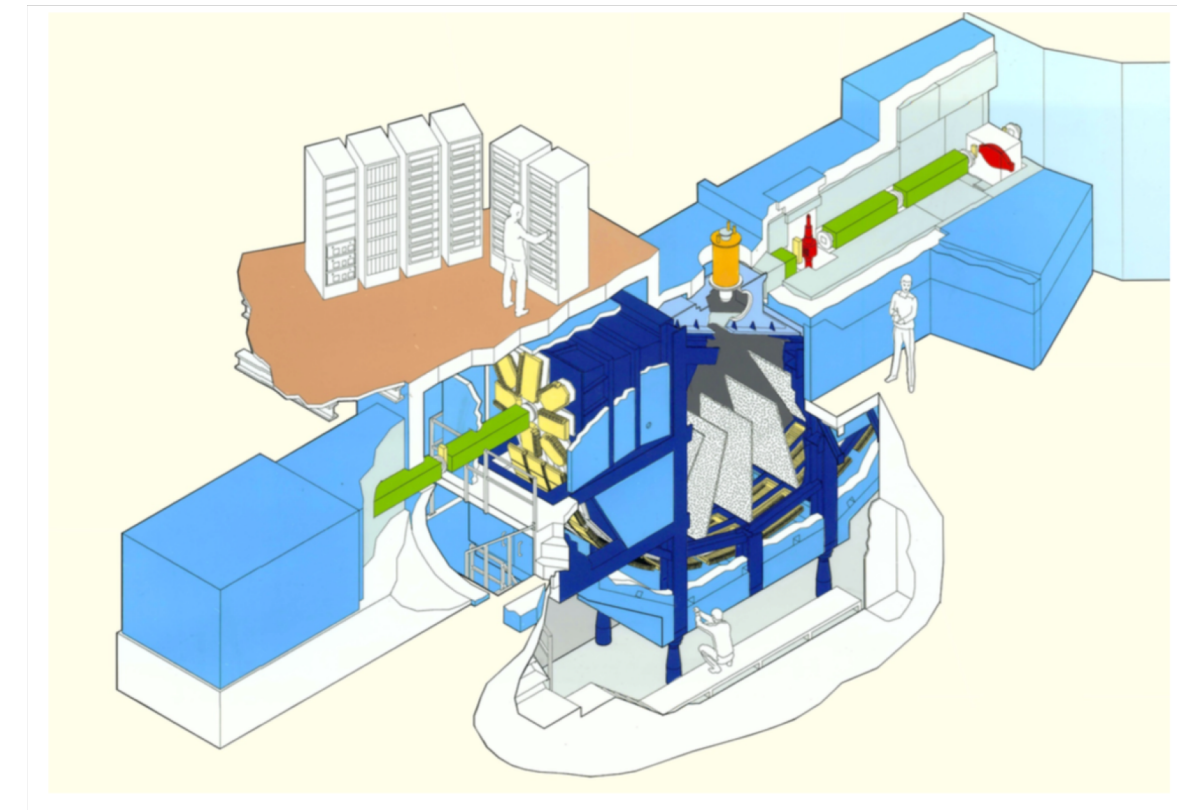
*McStas  
School*

*McStas*



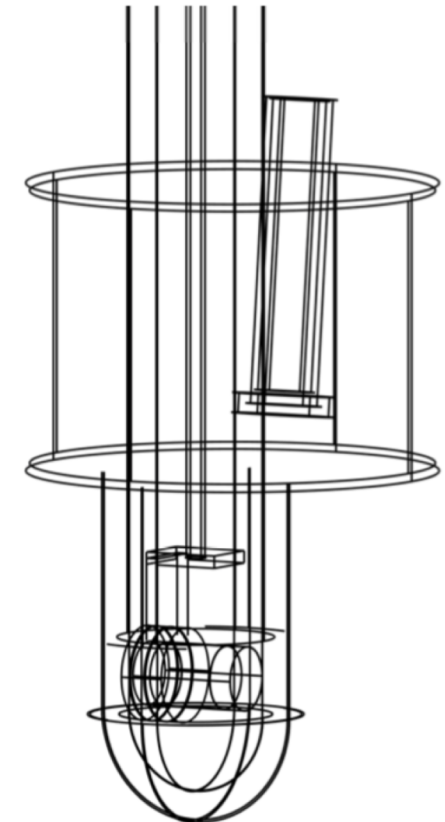
# My work on MARI @ ISIS

- Simulation of instrument and comparison to data
- Experiment performed by John Taylor and members from Kim Kefmanns group
- Time of flight data
- Powder spectrometer

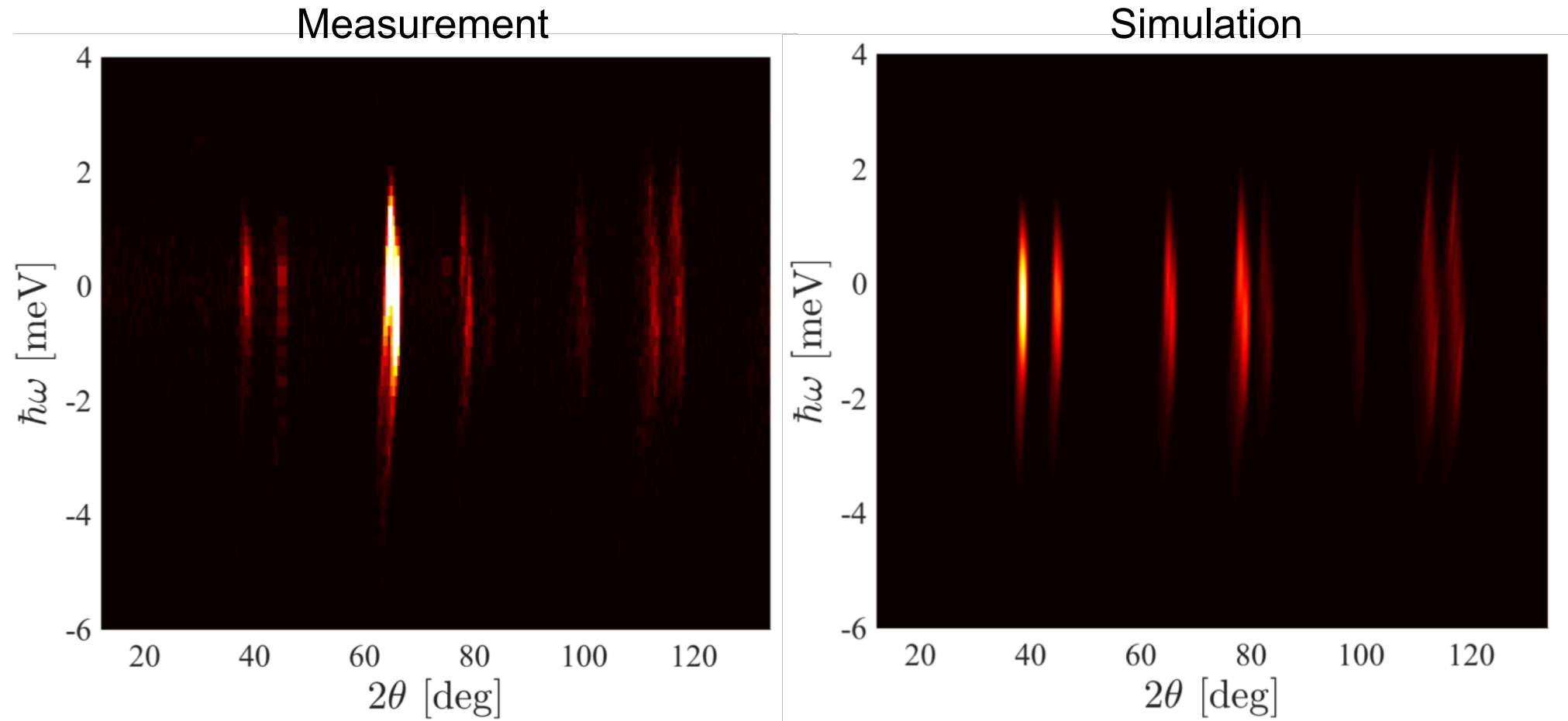


# Sample environment

- Detectors underneath sample environment
- Only lower part simulated

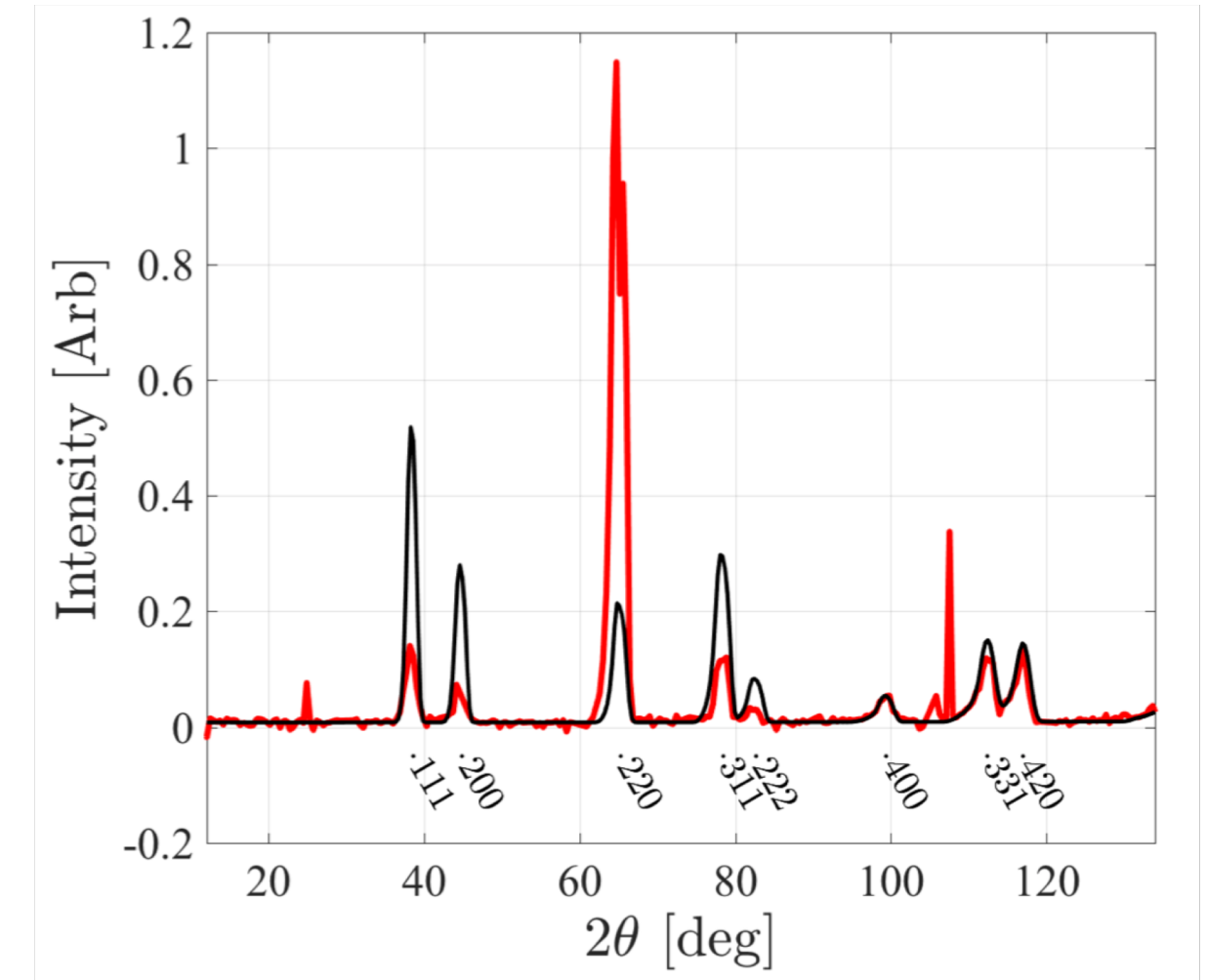


# Empty sample environment 35 meV beam

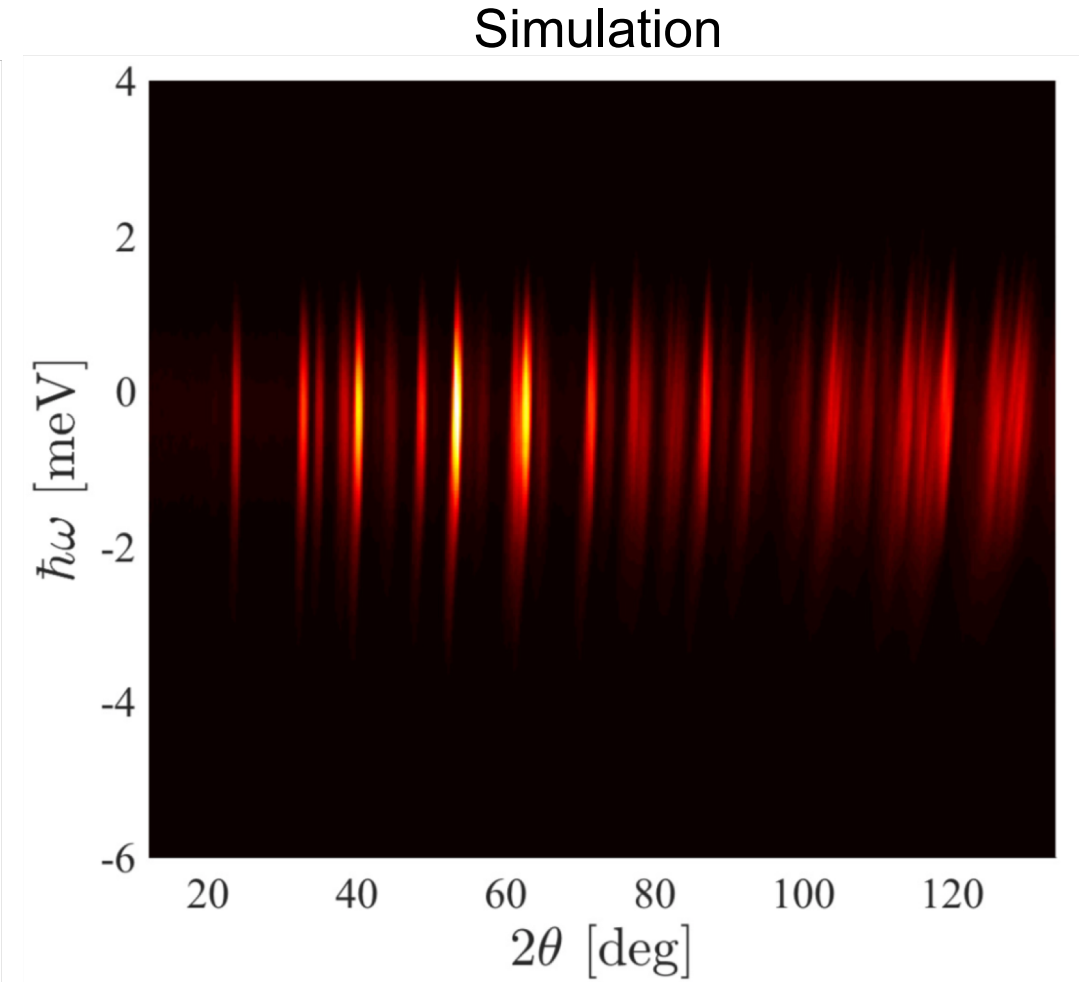
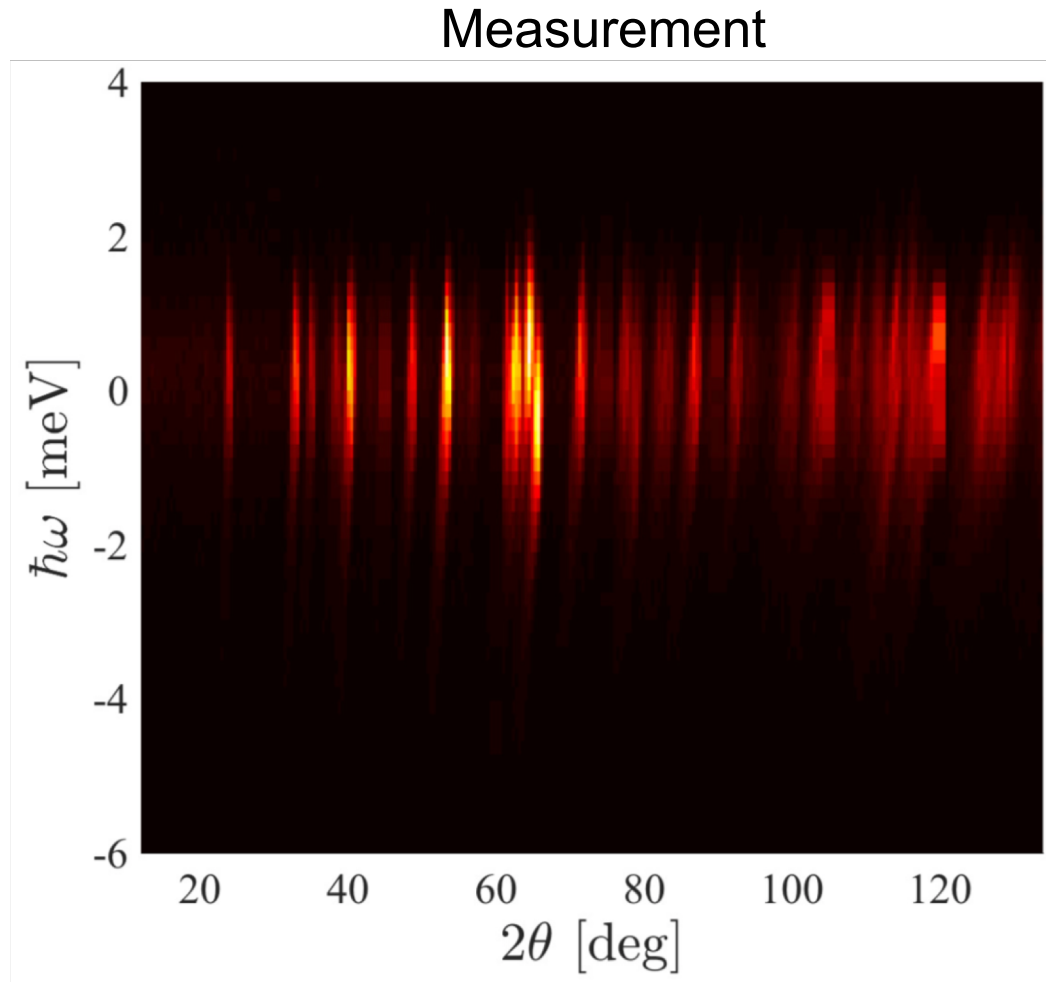


# Empty sample environment 35 meV beam

- Some issue with texture in cryostat, preferred orientations in the powder

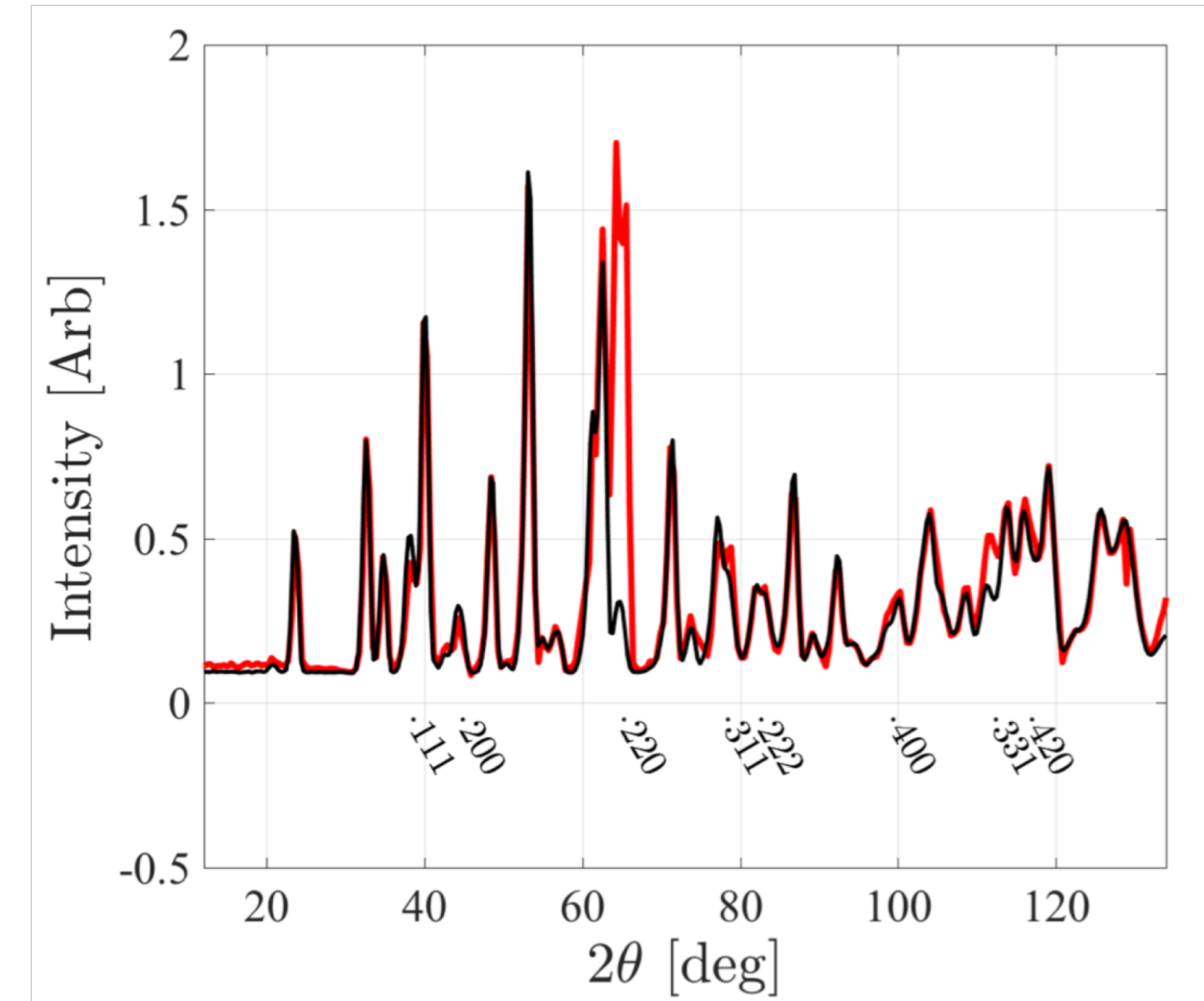


# With sample 35 meV



# With sample 35 meV

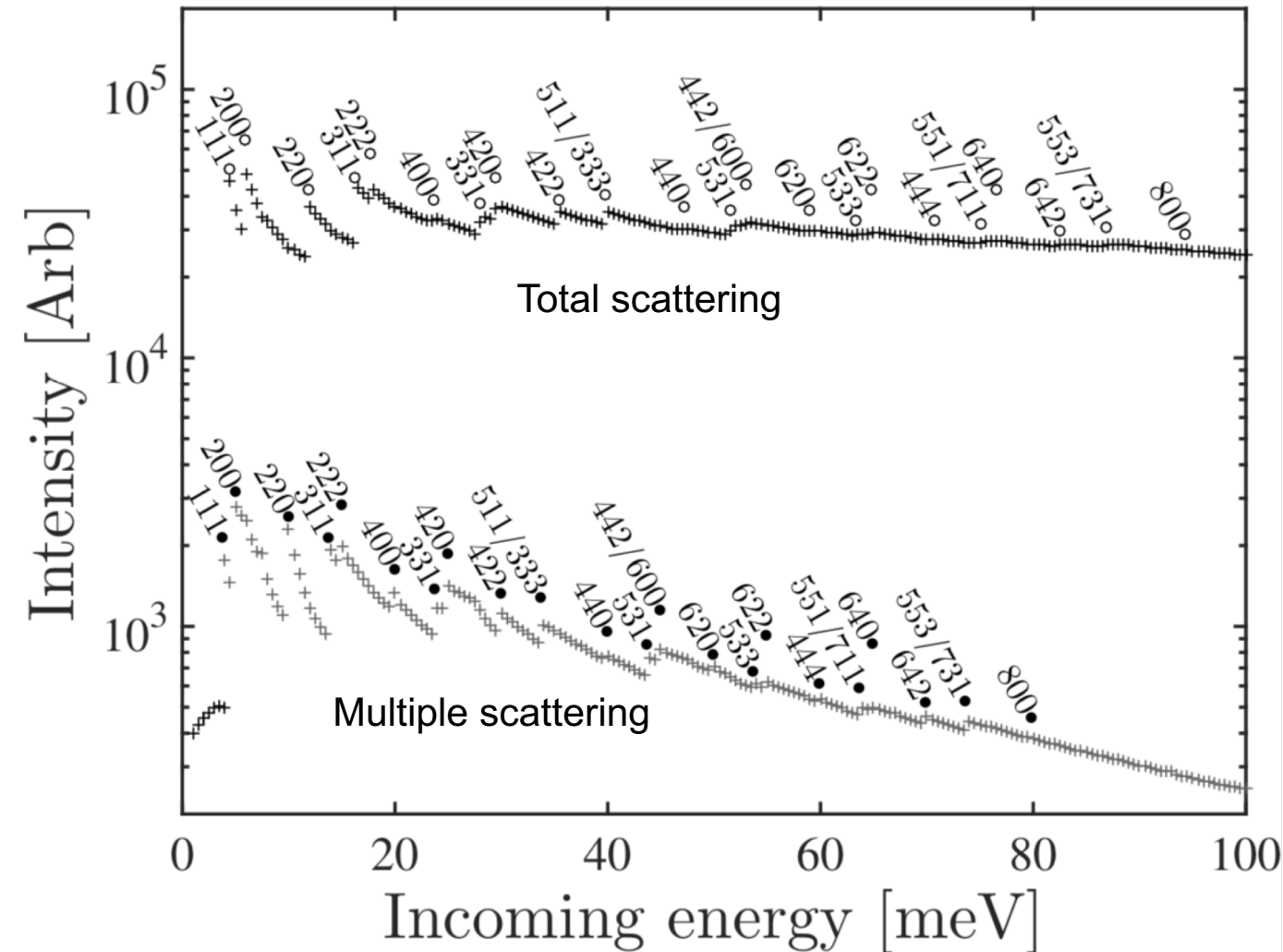
- Sample signal matches well
- Still issue from the empty cryostat



# Selecting best incoming energy

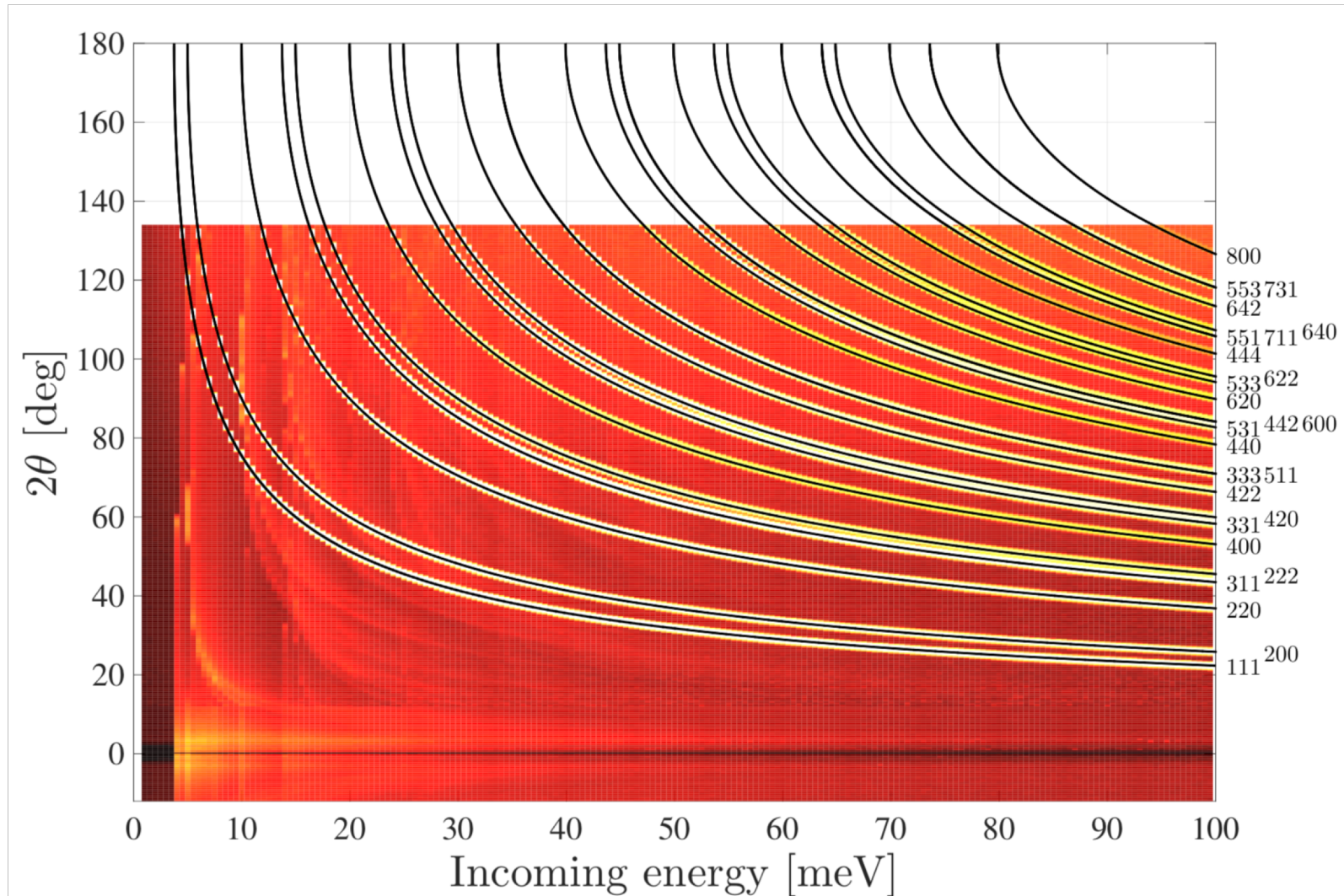
- Single scattering measured by instrument depend on detector coverage
- Multiple scattering depends on activation of Bragg reflections

- Bragg peak is at  $2\theta = 134$  deg
- Bragg peak is at  $2\theta = 180$  deg



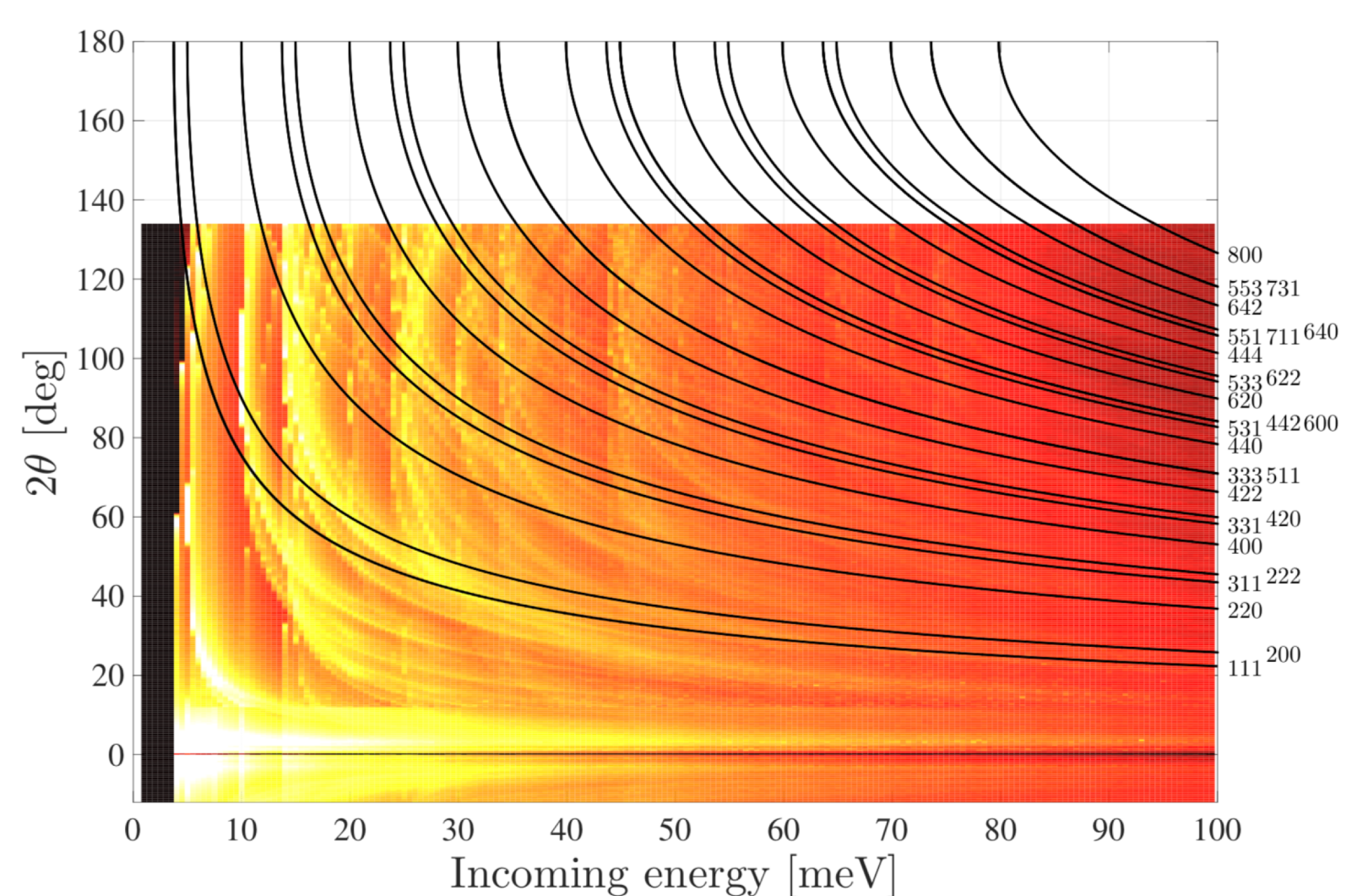
# Selecting best incoming energy

- Al powder lines



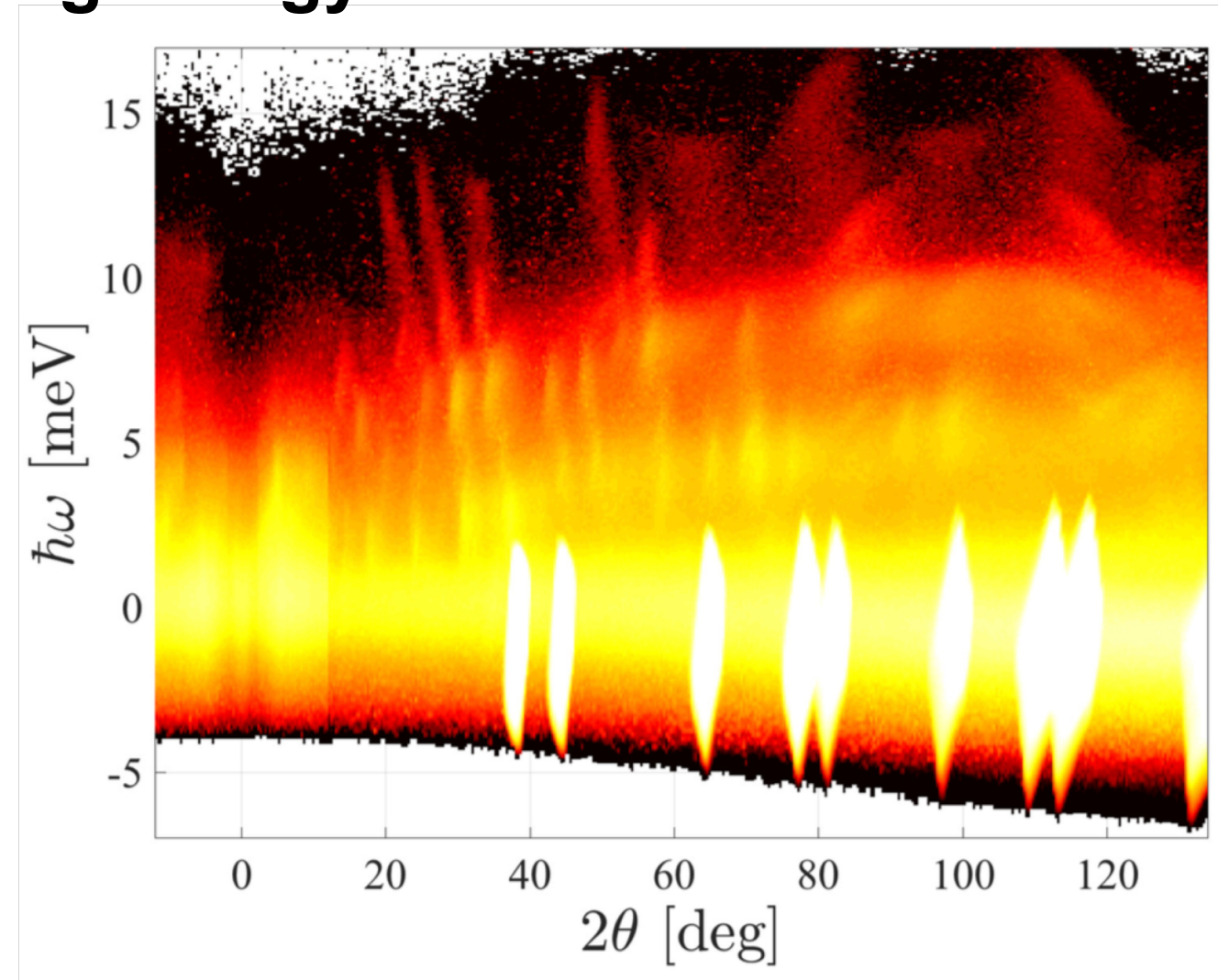
# Selecting best incoming energy

- Al powder lines
- Only multiple scattering



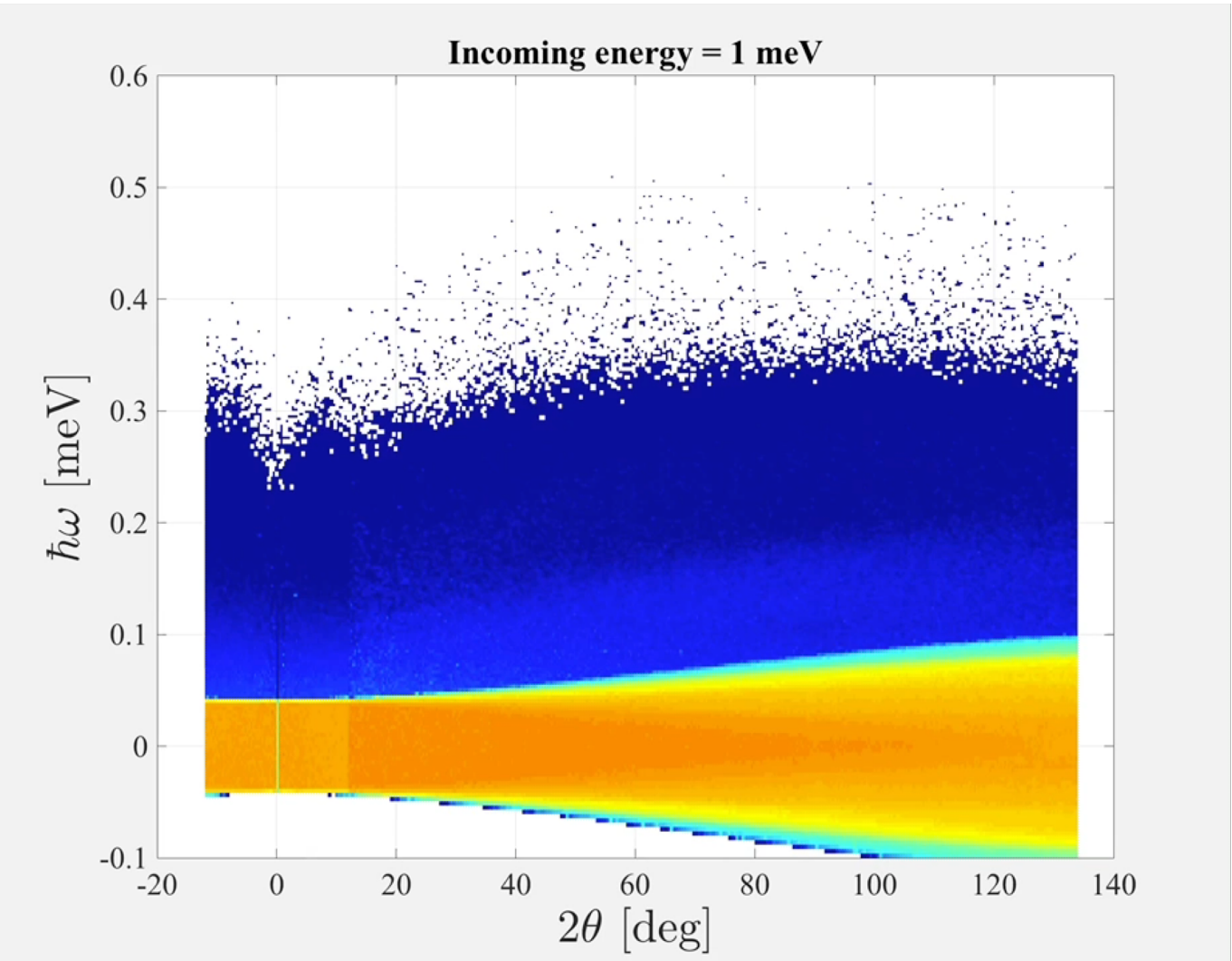
# Selecting best incoming energy

- Simulation of 35 meV
- Logarithmic scale 2 – 7 orders below Al powder bragg peaks



# Selecting best incoming energy

- Simulation of empty cryostat
- Range of incoming energies
- Showing resulting dataset



# Conclusions

- Difficult to simulate all aspects and get perfect agreement
- Simulation provides some important benefits when it is accomplished
- For example assistance in selecting the best settings for an instrument

2019 CSNS  
*McStas*  
*School*

